Molecular Acclimation of *Halobacterium salinarum* to Halite Brine Inclusions

C. Favreau[1], A. Tribondeau[2], M. Marugan[1], F. Guyot[3], B. Alpha-Bazin[4], A. Marie[1], R. Puppo[1], T. Dufour[5], A. Huguet[6], S. Zirah[1], A. Kish[1*]

[1]Unité Molécules de Communication et Adaptation des Microorganismes (MCAM), Muséum National d'Histoire Naturelle (MNHN), CNRS, 57 rue Cuvier, 75005 Paris; France

[2]Unité Physiologie Moléculaire et Adaptation (PhyMA), MNHN, CNRS, 57 rue Cuvier, 75005 Paris; France

[3]Institut de Minéralogie, de Physique des Matériaux et de Cosmochimie (IMPMC), MNHN, Sorbonne Université, CNRS, IRD, 4 place Jussieu, 75005 Paris; France

[4] Département Médicaments et Technologies pour la Santé (DMTS), Université Paris-Saclay, CEA, INRAE, SPI, 30200 Bagnols-sur-Cèze; France

[5]Laboratoire de Physique des Plasma (LPP), Sorbonne Université, CNRS, Ecole Polytechnique, Université Paris-Sud, Observatoire de Paris, 4 Place Jussieu, 75252 Paris; France

[6]Unité Milieux Environnementaux Transferts et Interactions dans les hydosystèmes et les Sols (METIS), Sorbonne Université, CNRS, EPHE, PSL 4 place Jussieu, 75005 Paris; France

*** Correspondence:**
Adrienne Kish, Unité MCAM, Muséum National d'Histoire Naturelle (MNHN), CNRS, 57 rue Cuvier, 75005 Paris; France
adrienne.kish@mnhn.fr

Keywords: *Halobacterium*, halophile, halite, proteomics

1 Abstract

Halophilic microorganisms have long been known to survive within the brine inclusions of salt crystals, as evidenced by their pigmentation. However, the molecular mechanisms allowing this survival has remained an open question for decades. While protocols for the surface sterilization of halite (NaCl) have enabled isolation of cells and DNA from within halite brine inclusions, "-omics" based approaches have faced two main technical challenges: (1) removal of all contaminating organic biomolecules (including proteins) from halite surfaces, and (2) performing selective biomolecule extractions directly from cells contained within halite brine inclusions with sufficient speed to avoid modifications in gene expression during extraction. In this study, we present methods to resolve these two technical challenges. In addition, we apply these methods to perform the first examination of the early acclimation of a model haloarchaeon (*Halobacterium salinarum* NRC-1) to halite brine

inclusions. Examinations of the proteome of *Halobacterium* cells two months post-evaporation revealed a high degree of similarity with stationary phase liquid cultures, but with a sharp down-regulation of ribosomal proteins. Low quantities of RNA from halite brine inclusions corroborate the hypothesis of low transcriptional and translational activities. While proteins for central metabolism were part of the shared proteome between liquid cultures and halite brine inclusions, proteins involved in cell mobility (archaellum, gas vesicles) were either absent or less abundant in halite samples. Proteins unique to cells within brine inclusions included transporters, suggesting modified interactions between cells and the surrounding brine inclusion microenvironment. The methods and hypotheses presented here enable future studies of the survival of halophiles in both culture model and natural halite systems.

2 Introduction

Extremely halophilic archaea are adapted to the highest possible salinity conditions, thriving in saturated brines. Microbial diversity in such environments is highly reduced and tends to be dominated by haloarchaea (Oren, 2006). Saturated brines are characterized by low dissolved oxygen content despite contact with the air and are often exposed to elevated temperatures and high levels of solar radiation (Oren, 2006; Merino *et al*., 2019) leading to evaporation. During evaporation events, the total contents of the brine, including salts, organics, some atmospheric gases, and any microorganisms present, are trapped within inclusions in the salt crystals. Viable halophilic bacteria and archaea have been isolated from halite (NaCl) of various ages, from months to years (Norton and Grant, 1988; Gramain *et al*., 2011; Huby *et al*., 2020), to geologically relevant timescales. Some studies have even reported the observation or isolation of microorganisms from halite dated to several hundreds of millions of years (Vreeland *et al*., 2000; Schreder-Gomes *et al*., 2022). These observations have raised two important questions: (1) are these truly 'ancient' cells? (2) what physiological changes are required for microbial cells to remain viable within halite brine inclusions?

The first question has been studied in greater detail, and while many questions still remain, these studies provided valuable insights into the potential for surface-contaminant microorganisms (Graur and Pupko, 2001; Maughan *et al*., 2002; Nickle *et al*., 2002). In response to these criticisms, appropriate surface sterilization and cleaning procedures for microbial cultivation and DNA isolation for micro-biodiversity studies from dissolved ancient halite (Gramain *et al*., 2011; Sankaranarayanan *et al*., 2011) were developed. These approaches enabled more accurate identification of only those microorganisms trapped within halite inclusions. Another opened question is whether the age

determined from the mineral halite can be applied directly to the microorganisms in the brine inclusions. Some studies have examined the possibility that microbial cell-like biomorphs are preserved within brine inclusions (Nims *et al*., 2021).

Experimentally confirming how microbial life is supported within brine inclusions has proven more difficult. Determining the cellular functions expressed by viable halophiles within halite brine inclusions requires the direct isolation of biomolecules such as proteins and nucleic acids for "-omics" analyses, including proteomics and transcriptomics. However, significant technical challenges are presented by the closed system of brine inclusions within halite. Accessing the contents of brine inclusions by rapid crystal dissolution leads to cell lysis by osmotic shock and biomolecule degradation, while the time required for gradual crystal dissolution preserving cellular integrity is also sufficient for alterations in the transcriptomes and proteomes of viable cells away from their state within the brine inclusions. In addition, the direct extraction of biomolecules from brine inclusions involves a large amount of NaCl, which is incompatible with mass spectrometry due to the lack of sufficient desalination steps. Although current hypotheses concerning the modifications of halophile physiology during entrapment within halite brine inclusions include a change to anaerobic metabolism (Winters *et al.,* 2015) along with potential for cell envelope modifications depending on conditions (Fendrihan *et al*. 2012; Kixmüller *et al*., 2012), these remain largely unverified at the molecular level due to these experimental challenges. New methods are needed to isolate proteins and RNA directly from halite brine inclusions, without allowing the microorganisms to alter their gene expression during salt dissolution and processing. The development of a new analytical workflow compatible with multi-omics analyses is best conducted with a known model organism for which there is a large repertoire of physiological studies and multi-omics data for liquid cultures exposed to a range of conditions applicable to halite brine inclusions (different oxygen availabilities, salinities, nutrient availabilities, etc.). For these reasons, we choose the model haloarchaeon *Halobacterium salinarum*, the type strain of the *Halobacteriales* family (Gruber, 2004; Oren, 2009).

H. salinarum is an appropriate model as it is found both in contemporary NaCl-saturated aqueous environments such as Great Salt Lake (Post, 1977) and has been detected in halite and closely related to isolates from ancient salt deposit (Mormile *et al*., 2003). The accumulation of high intracellular concentrations of potassium (K^+) and chloride (Cl^-) (Engel and Catchpole, 2005), needed to maintain osmotic homeostasis, induces both biochemical adaptations (in the form of a strongly acidic proteome) as well as technical challenges to desalt cellular extracts. *H. salinarum* survives in changing

environments by using a complex variable energetic metabolism with a preference for aerobic respiration but capable to switch under low oxygen conditions to phototrophy via bacteriorhodopsin, arginine fermentation or anaerobic respiration using dimethyl sulfoxide (DMSO) and trimethylamine oxide (TMAO) if available (Hartmann *et al*., 1980; Müller and DasSarma, 2005; Falb *et al*., 2008; Gonzalez *et al*., 2009). Established multi-omics protocols for liquid cultures of *H. salinarum* have permitted analyses of the cellular responses to a broad range of environmental conditions, including variations in NaCl (Leuko *et al*., 2009), pH (Moran-Reyna and Coker, 2014), oxygen (Schmid *et al*., 2007), and temperature (Coker *et al*., 2007), all relevant to halite brine inclusions. This existing knowledge base far exceeds that developed to date for halophiles isolated directly from ancient halite. Using the established techniques and known physiological responses of liquid cultures *H. salinarum*, we were able to develop new analytical techniques.

Here we present this new toolkit for the study of microorganisms within halite, validated using *H. salinarum* entrapped in lab-grown halite to answer the question of what physiological changes are required for microbial cells to remain viable within halite brine inclusions, focusing on the initial phase of halite entrapment. The workflow developed includes removal of not only surface-attached cells and nucleic acids but also proteins, with subsequent extraction and desalting of proteins directly from brine inclusions compatible with mass spectrometry analyses. Applying these methods, we determined the molecular acclimation of *H. salinarum* cells to inclusions within lab-grown halite by analyzing the differences in the expressed proteome prior to evaporation and two months after culture evaporation. Analyses focused on the characterization of cellular activity compared to stationary cells not trapped within halite, as well as the interactions of cells with halite brine inclusion environment.

3 Material and Methods

All reagents used were analytical grade and suitable for molecular biology.

3.1 Strain and Culture Conditions

Halobacterium salinarum strain NRC-1 (JCM 11081) was grown under oxic conditions in autoclaved complex medium (CM: 4.28 M NaCl, 81 mM $MgSO_4.7H_2O$, 27 mM KCl, 10 mM trisodium-citrate.$2H_2O$, 1 % (w/v) peptone Oxoïd® LP0034, pH adjusted to 7.4) following Oesterhelt and Stoeckenius, 1974 at 37 °C, 180 rpm. Growth was monitored by spectrophotometry at 600 nm (OD_{600}). Cultures for crystallizations, proteins and RNA extractions were grown to stationary phase (OD_{600} =

1.0 to 1.6) to approximate the physiological condition of haloarchaea under natural conditions during evaporation.

3.2 Laboratory-Grown Halite

3.2.1 Internally Inoculated Halite

Modeling entombment of haloarchaea within halite was already done in laboratory by Norton and Grant (1988), Gramain *et al*. (2011) and Kixmüller *et al*. (2012). In this study, laboratory-grown halite crystals were produced following a modified version of protocols of Fendrihan *et al.* (2012), by adding nutrients to their Tris-buffered NaCl solution (TN buffer; 100 mM Tris-HCl pH 7.4, 4.28 M NaCl) to simulate cell lysis and metabolite release from less extreme halophiles concomitant with increasing NaCl concentrations in the natural environment just prior to halite precipitation (Winters *et al.*, 2015). Briefly, *H. salinarum* cells in stationary growth phase were harvested by centrifugation at 7 500 x g, 10 min, 20 °C and the growth medium removed by washing with sterile TN buffer. Cells were then resuspended in sterile TNPA buffer (TN buffer with 1 % (w/v) Oxoïd® peptone LP0034 and 0.5 % (w/v) L-Arg HCl, adjusted pH 7.4) with a ratio of 10 mL TNPA buffer per 500 mg of cells (wet weight). A 20 mL volume of cell resuspension was evaporated in each sterile 90/14.3 mm Petri dish in a 37 °C with a 12 h:12 h light:dark photoperiod (66,75 µmol photons.m^{-2}.s^{-2}, verified by a Li-250A, Li-Cor Inc., Germany) to model natural brine-surfaces. Complete evaporation and drying of precipitated halite were obtained after ~22 days, followed by a further 60 days (two months) of incubation to study the early phase of *H. salinarum* entombment within halite brine inclusions.

3.2.2 Externally Inoculated Halite

To produce halite with *H. salinarum* cells localized exclusively at the halite surface, 20 mL of sterile TN buffer was first evaporated as described above until complete drying (~ 22 days). The resultant crystals were then collected aseptically using sterilized forceps and inoculating the surfaces of each crystal with 4.5×10^9 *H. salinarum* cells in stationary phase, applied as a highly concentrated cell solution after centrifugation (7 500 x g, 10 min, room temperature, RT°C). Crystals were inoculated on the largest faces (designated here as 'top' and 'bottom', see Figure 2k) by first inoculating the 'top' face drop-by-drop and spreading out using a sterile inoculating loop. Halite were then dried overnight at 37 °C, followed by the 'bottom' face the next day with the same protocol.

3.3 Scanning Electron Microscopy (SEM)

Observations and analyses of evaporite crystals were performed by first attaching the halite directly to aluminum supports with carbon tape followed by carbon coating (7-8 nm thickness). Observations were performed using a Zeiss Ultra 55 field emission gun scanning electron microscope (SEM-FEG) equipped with a Brucker EDS QUANTAX detector installed at IMPMC (Sorbonne Université, Paris, France). Secondary electron images were obtained using an in-column detector (InLens) at 10 kV and a working distance of 7.5 mm. Energy dispersive X-ray spectroscopy (EDX) analyses and mapping were performed at 15 kV at a working distance of 7.5 mm.

3.4 In-Brine Cellular Viability Tests

To assess cell viability after halite inclusion, salt crystals were weighted to determine the appropriated NaCl concentration required for the complex medium to obtain a final concentration of 4.28 M after halite dissolution as previously described by Gramain *et al.* (2011). Halite and complex medium were then incubated at 37 °C, 180 rpm. After crystal dissolution, cultures were visually inspected then OD_{600} and morphology by optical microscopy was measured. Red colored cultures reaching a normal stationary phase culture ($OD_{600} > 1.0$) were classified as viable and cultures showing no increase in OD_{600} after 1 month ($OD_{600} < 0.1$) were classified as non-viable.

3.5 Halite Surface Cleaning (Removal of Cells and Proteins)

3.5.1 Cold Atmospheric Plasma Treatment

Cold atmospheric plasmas (*i.e.*, weakly ionized gases) were generated were generated using either a dielectric barrier device (DBD) or an atmospheric pressure plasma jet (APPJ). They were polarized to the high voltage using two types of electrical power supply: (1) an alternative current (AC) generator composed of a function generator (ELC, GF467AF) and a power amplifier (Crest Audio, CC5500) as well as (2) a pulse generator (RLC electronic Company, NanoGen1 model) coupled with a high voltage power supply (Spellman company, SLM 10 kV 1200W model). DBD and APPJ were supplied with different a carrier gas (helium or argon) with/without oxygen. Hence several plasma conditions were performed to produce active species (radicals, reactive oxygen species but also electrons and photons). The Table 1 details the experimental plasma conditions that were investigated as well as the resulting proteolysis to assess the efficiency of proteins removing.

3.5.2 Chemical Treatments

Previous studies applied surface cleaning protocols developed for removal of cells and nucleic acids, as detailed in Supplementary Table 1. To adapt these protocols for the removal of surface-bound proteins, we modified the protocol of Sankaranarayanan *et al*. (2011) using shorter time for baths to avoid dissolution of smaller laboratory-grown crystals. Briefly, crystals were incubated in successive 5 min baths: 4.00 - 4.99 % NaOCl (Honeywell Research Chemicals; avoiding commercial bleach solutions that induced rapid and near-complete crystal dissolution) in saturated NaCl and 10 M NaOH in saturated NaCl supplied or not with 10 N HCl followed by 100 mM Na_2CO_3 in saturated NaCl. A sterile saturated NaCl was used to wash off each treatment solution between each successive bath, testing both passive wash baths and active-spray washes using a hemolytic pump.

3.6 Protein Extraction and Preliminary Desalting

All solvents used for protein extractions were HPLC-grade and suitable for mass spectrometry analysis. Extractions were performed with TRIzol Reagent™, based on the halophilic protein extraction protocol of Kirkland, *et al*. (2006). This protocol was modified for protein extraction directly from halite crystals with high salt content and proteomics analysis by mass spectrometry. Compatibility for liquid cultures was kept as described below. All steps described were performed with autoclaved glassware to avoid any organics contamination from plastics (bench top protocol see Supplementary Section 2). Briefly, crystals were fully immersed in 5 mL of TRIzol Reagent™ in 30 mL glass centrifuge tube and crushed using autoclaved glass stir-rod. After 20 min incubation at 60 °C, total RNA was extracted from the resulting cell lysate by adding 1 mL of 100 % chloroform, incubating for 5 min at RT°C followed by phase separation by centrifugation (10 000 x g, 20 min, 4 °C). The chloroform-containing aqueous phase was removed with autoclaved glass Pasteur pipet and 1.5 mL of 100 % ethanol was added to precipitate DNA. After 3 min at RT°C, supernatant was collected by centrifugation (2 000 x g, 10 min, 4 °C). Proteins were precipitated with 7.5 mL of 100 % isopropanol and collected by centrifugation (10 000 x g, 20 min, 4 °C). The resulting protein pellet was washed twice to remove phenol traces using 5 mL of 0.3 M guanidine-HCl in 95 % ethanol to denature the proteins, followed by a third wash step with 5 mL of 100 % ethanol to remove any residual guanidine-HCl. Each wash step was performed by incubating the cell pellet in the solution for 20 min at RT°C followed by centrifugation (10 000 x g, 20 min, 4 °C). Protein desalting was accomplished by two successive protein precipitations with 2 mL of 100 % glacial acetone (-20 °C) and centrifugation (10 000 x g, 20 min, 4 °C). After acetone removal, the pellet was completely dried under laminar flow. Then, proteins were solubilized in 1 M

209 $NaHCO_3$ with 0.1 % SDS at RT°C for two days and quantified with a bicinchoninic acid (BCA)
210 proteins assay (Pierce) using bovine serum albumin (BSA) standards concentration from
211 manufacturer's instruction in the case of quantitative mass spectrometry and adapted BSA standard
212 concentrations (enable low protein concentration assay, see Supplementary Section 3) for surface
213 proteins removal procedure. Proteolysis rate was determined by proteins quantity comparison with and
214 without treatments.

215 Total proteins were extracted from *H. salinarum* cultures in stationary growth stage using the
216 same procedure. For this, 2.0 $x10^{10}$ cells from liquid cultures were pelleted by centrifugation (7 500 x
217 g, 10 min, 20 °C) and the cell pellets directly resuspended in 5 mL TRIzol Reagent™ solution, prior
218 to following all steps described above for halite samples. After solubilization of the protein pellet,
219 solubilization with 1M $NaHCO_3$ with 0.1 % SDS at RT°C, protein quantification was performed using
220 the BCA assay (Pierce) protein assays as per the manufacturer's instructions.

221 **3.7 iTRAQ® Isobaric Labelling and Mass Spectrometry**

222 Aliquots of 100 µg of proteins for each sample condition and replicate were reduced using 2 mM of
223 tris-(2-carboxyethyl) phosphine (TCEP) at 37 °C for 1 h, and alkylated with 5 mM of iodoacetamide
224 30 min in the dark at RT°C prior to digestion with 5 µg of trypsin Gold (Promega) for 15 h at 37 °C.
225 After digestion, peptides were directly desalted by solid phase extraction (SPE) using C18 cartridges
226 (Sep-Pak C18 Plus Short 400 mg Sorbent, Waters). The resulting peptides were dried by speed-vac
227 and resuspended in tetraethylammonium bromide (TEAB) 0.5 M prior to labelling. iTRAQ® labelling
228 was performed according manufacturer's instructions (Applied Biosystems). Briefly, each of the
229 iTRAQ® isobaric labelling reagents were reconstituted with isopropanol and then added to the 50 µg
230 of protein digest (113, 114, 115 and 116 iTRAQ® isobaric labels for proteins from liquid controls and
231 117, 118, 119 and 121 for halite brine inclusion protein extractions). After 2 h at RT°C, samples were
232 desalted again with C18 SPE. The labelled peptides eluted were then dried by speed-vac and
233 resuspended in 2 % acetonitrile, 98 % H_2O with 0.1 % formic acid, see Supplementary Section 5.

234 Labelled peptide samples were analyzed by mass spectrometry as previously described (Pinel-
235 Cabello *et al.,* 2021) on a Q Exactive HF tandem mass spectrometer (Thermo Scientific) coupled to an
236 UltiMate 3000 Nano LC System. Peptides were desalted online on an AcclaimPepmap100 C18
237 precolumn (5µm, 100 Å, 300 µm i.d x 5 mm) and further resolved on a nanoscale AcclaimPepmap100
238 C18 column (3 µm, 100 Å, 75 µm i.d. x 500 mm) at a flow rate of 200 nL min^{-1} using a 120-min

239 gradient of 4-32% acetonitrile. A Top 20 strategy was applied in data dependent acquisition mode. Full
240 scan mass spectra were acquired from 350 to 1800 *m/z* at a resolution of 60,000 with an automatic gain
241 control (AGC) target set at 3 $\times 10^6$ ions. MS/MS fragmentation was initiated when the ACG target
242 reached 10^5 ions with an intensity threshold of 9×10^4. Only precursor ions with potential charge states
243 of 2^+ and 3^+ were selected for fragmentation applying a dynamic exclusion time of 10 s.

244 3.8 Mass Spectrometry Data Analyses

245 3.8.1 Protein Identification

246 Protein identifications were performed using PEAKS® X-Pro software (64 bits version, 2020,
247 BioInformatics solutions). It allows database search assisted *de novo* sequencing against the protein
248 coding sequences from *H. salinarum* NRC-1 (8 533 entries from NCBI, downloaded 2021/08/03).
249 MS/MS assignment was searched with the following parameters: (1) mass tolerance of 10 ppm on the
250 parent ion, (2) mass tolerance of 0.005 Da for fragment ions from MS/MS; (3) carbamidomethylated
251 Cys (+57.0215) and iTRAQ® isobaric tag Lys and N-terminal (+304.2054) as static modifications; and
252 (4) oxidized Met (+15.9949), deamidated Asn and Gln (+0.9840) and iTRAQ® isobaric tag Tyr
253 (+304.2054) as variable modification. The false discovery rate (FDR) was estimated with decoy-fusion
254 option.

255 Then, resulting proteins lists were then filtered allowing FDR < 1 % (corresponding to a -
256 10logP score above 25) for peptide-spectrum matches (PSMs), protein identification using minimum
257 2 unique peptides per proteins (a unique peptide is a peptide with a -10logP score above the peptide
258 filtering threshold that can be mapped to only one protein group).

259 3.8.2 Protein iTRAQ® Quantitation

260 The eight labelled samples (four replicates each of proteins from liquid stationary cultures and from
261 halite brine inclusions) were mixed in equimolar ratios and injected in nanoLC-MS/MS in triplicate to
262 reduce instrument variability. Quantitation was performed using PEAKS Q (quantitation program)
263 iTRAQ 8-plex type with 10 ppm mass tolerance and only peptides with a score above FDR threshold
264 1 % are used to quantify the identified proteins. Resulted quantitation was filtered accepting only
265 proteins groups with fold change ≥ 2, at least two unique peptides and FDR adjusted ≤ 1 % for both
266 proteins identification and fold change significance using ANOVA significance method. Mass
267 spectrometry proteomics data have been deposited to the ProteomeXchange Consortium via the PRIDE
268 partner repository with the dataset identifier (*under submission*).

3.8.3 Sample Comparisons and Functional Annotation

Potential biases during analysis were avoided by filtering protein identifications produced using the PEAKS software to group proteins having multiple annotations in the NCBI database. To do so, we developed custom BASH and PYTHON scripts to merge all descriptions for one proteins identifier (favoring in order AAG-type, DAC-type, WP-type and then Q9H-type identifier). Venn diagrams were computed with VennDiagram and ggplot2 packages in R script. Functional proteins annotation was done with Kyoto Encyclopaedia of Genes and Genomes (KEGG, Kanehisa and Goto, 2000) using blastKOALA tool (Kanehisa *et al*., 2016; https://www.kegg.jp/blastkoala/), assigning K numbers to identified proteins (see Supplementary Table 6-2). K number were then used for mapping identified proteins onto pre-existing metabolic pathways using KEGG Mapper search tools (https://www.kegg.jp/kegg/mapper/search.html ; see Supplementary Table 6-3).

3.9 Total RNA extraction and analysis

Total RNA for transcriptomics analyses were extracted using TRIzol Reagent™ method described above for protein extractions with the following modifications. To avoid RNA degradation, the TRIzol Reagent™ mixture with pulverized halite crystals was incubated for 5 min at RT°C rather than 20 min at 65 °C. The chloroform phase was then collected by centrifugation and RNA purification was perform using RNeasy MinElute cleanup columns (Qiagen). Resulting RNA were quantified using QuBit Q32857 (Invitrogen) the purity assayed using Nanodrop 2000/2000c (Thermo Scientific), and the quality was determined with the BioAnalyzer 2100 system (Agilent). All steps after RNA extraction were performed according manufacturer's instructions with RNAase-free materials and solutions.

4 Results

4.1 Characterization of Laboratory-Grown Halite Containing *H. salinarum*

In order to study the physiology of *H. salinarum* cells after entombment within brine inclusions, we first needed to characterize the laboratory-grown halite, including resultant crystal size, cell localization, and surface-bound biomolecules. This enabled the establishment of selection criteria for downstream proteomics analyses and the development of protocols to exclude any 'contaminant' proteins from the surface of the crystal.

4.1.1 Variability of *H. salinarum* cells from Inoculated Laboratory-Grown Halite

Laboratory-grown halite crystals produced from TNPA solutions containing *H. salinarum* cells using a slow evaporative process exhibited heterogeneous crystallization with respect to crystal size and

coloration. As shown in Figure 1, even replicates produced under the same conditions produced different quantities of crystals of varying lengths and widths, but with relatively uniform thicknesses (±1 mm) of hopper and fishtail crystals. Color variations observed for halite in this study were likely the result of heterogeneities in the number of brine inclusions containing pigmented *Halobacterium* cells. The red color indicative of *H. salinarum* cells tended to concentrate in the center of hopper crystals where inclusions were most abundant (Roedder *et al*., 1984). Individual crystals of similar size and coloration were collected aseptically for further study, selecting only halite without visible defects signaling potential rupture of near-surface brine inclusions.

4.1.2 Contaminating Surface-Bound Cells and Proteins

To evaluate the potential for 'contaminating' microbial cells or residual biomolecules at the crystal surface, the elemental composition of halite with and without *H. salinarum* cells were determined by SEM-EDX. Elemental analyses of control halite derived from evaporation of the TNPA solution only exhibited the expected sodium chloride crystal surface, along with dense, irregular C agglomerates (Figure 2c-f) derived from the presence of organics (peptone, L-Arg) in the TNPA solution. The addition of *H. salinarum* cells to the TNPA solution prior to evaporation produced similar structures to control crystals, with no intact cells of *H. salinarum* visible on halite surfaces (Figure 2i,j). However, EDX analyses revealed differences in the distribution of carbon compared to control samples, as well as the presence of microscopic potassium crystals at the halite surface (Figure 2j). These differences were likely due to lysis of surface adhered *H. salinarum* cells releasing high concentration of cytosolic K^+ and Cl^- accumulated as part of the "salt-in" osmoadaptation strategy. In order to assess both the potential for surface bound contaminants, including viable cells as well as proteins, externally inoculated halite were produced (Figure 2k). After two months incubation, halite surface-attached cells were revealed to be (at least partially) viable according positive viability test. After growth back, culture observations by optical microscopy showed rod-shaped cells with low motility. Additionally, SEM-EDX analysis of externally inoculated crystals revealed a similar elemental composition and distribution to that of internally inoculated halite (bearing cells both within brine inclusions as well as on the halite surface) after two months post-evaporation (Figure 2m,n). Taken together, these results confirm the presence of both viable cells and cellular debris on the surface of halite after two months of desiccation, validating the need for halite surface cleaning procedure to remove any residual proteins.

4.2 Development of Total Protein Isolation Methods for Halite

330 For proteomics approaches inside crystals without prior dissolutions, a new methodology for direct
331 proteins extraction from brine inclusions was developed. This method was based on the protocol of
332 Kirkland *et al*. (2006) for liquid cultures to allow mass spectrometry analysis compatible both for
333 crystals and liquid cultures with TRIzol Reagent™ (see Supplementary Section 4 for details on the
334 parameters tested during protocol development and optimization). Briefly, protocol was modified to
335 optimize desalting steps (due to direct halite extraction with high NaCl content), proteinaceous pellets
336 dissolution and proteinaceous digestion.

337 **4.3 Development of Proteolysis Protocols for Removal of Halite Surface-Bound Contaminants**

338 Previous halite cleaning procedures from Gramain *et al*. (2011) and Sankaranarayanan *et al*. (2011)
339 (see Supplementary Table 1) were developed to deactivate surface-contaminating microorganisms and
340 remove surface-contaminating DNA. However, these methods were not designed for the removal of
341 other types of biomolecule contaminants, such as proteins. A new, modified surface cleaning procedure
342 was therefore needed to remove surface protein contamination to enable extraction of proteins only
343 from within halite brine inclusions while avoiding crystal dissolution during the cleaning process. To
344 meet these requirements, both cold plasma treatments and chemical protocols were tested using
345 externally inoculated halite.

346 Cold plasma exposure is routinely used in astrobiology to sterilize spacecraft surfaces of
347 microbial contaminants prior to launch. For this reason, a cold plasma approach was investigated here
348 for the decontamination of halite surface. Two plasma sources – a DBD and an APPJ – were tested as
349 an alternative to conventional liquid solvents. The expected benefit was to minimize halite dissolution-
350 recrystallization events, hence ensuring the survival of the microorganisms within the halite. However,
351 owing to their insulating properties and irregular topography, halite crystals attenuate plasma electric
352 field and/or bend its field lines. As a result, and whatever the implemented plasma treatment (Ar, He,
353 He mixed with O_2), the externally inoculated halite crystals still retained the pink coloration which is
354 indicative of the protein and lipid pigments of *H. salinarum* cells (data not shown). As shown in Table
355 1, the most efficient plasma treatment drove to partial cell lysis (as determined by culture-based
356 viability tests following growth by OD_{600}) and to a proteolysis of only 39.1%: a value that remains
357 insufficient for the application.

358 As an alternative, chemical treatments were tested, using protocols modified from the
359 microorganism deactivation and DNA removal treatments of Sankaranarayanan *et al*. (2011) to extend
360 to proteolysis. First, reduction of the exposure times in each chemical bath from previously published

361 protocols were tested to avoid crystal dissolution, while maintaining the use of NaCl-saturated
362 chemical solutions to avoiding crystal dissolution. Subsequent, 5-minute sequential NaOCl and NaOH
363 treatments, either with or without additional HCl treatments, resulted in insufficient halite surface
364 proteolysis (Supplementary Figure 5-1a). This was likely due to the rough structure of hopper crystals,
365 which could allow proteins to remain attached during passive chemical baths. After chemical
366 treatments have partially degraded the contaminating biomolecules and reduce their attachment to the
367 halite surface, active-spray was used for wash steps to increase the efficiency of biomolecule removal
368 and prevent re-association with halite surfaces, compared to the use of passive wash baths
369 (Supplementary Figure 5-1b). Externally inoculated halite post-treatments with and without active-
370 spray, present reduced coloration. This active-spray method also allowed for both deactivation of halite
371 surface-bound microorganisms (as indicated by a lack of culture growth in post-treatment viability
372 tests) and better protein lysis compared to passive chemical bath washes. Using the protein extraction
373 method described above, the efficacy of active-spray method for removal of surface-bound proteins
374 was tested comparing NaOCl-NaOH and NaOCl-NaOH-HCl protocols. A shown in Figure 3a, addition
375 of an acid wash results in a proteolysis efficiency of 93.0 ±4.3 %, compared to from of 83.7 ±15.9 %
376 without the HCl treatment step (residual proteins 51.6 ±31.6 µg and 120.5 ±117,6 µg, respectively,
377 n=3). These results suggest that NaOCl-NaOH-HCl active-spray washes protocol (Figure 3b) present
378 optimal and less variable surface proteolysis for the case of this study, working on small laboratory-
379 grown halite crystals.

380 To ensure that this active-spray chemical treatment did not affect *H. salinarum* cells within the
381 halite brine inclusions, growth was monitored for crystals containing cells trapped in brine inclusions
382 after surface chemical cleaning with active-spray NaOCl-NaOH-HCl treatment. Viable cultures were
383 obtained from dissolution of the crystals in CM growth medium, thereby validating the active-spray
384 chemical surface protein removal protocol for use in studying biomolecules within halite brine
385 inclusions.

386 These new methods for removal of surface-bound proteins followed by extraction of total
387 proteins from halite brine inclusions using a modified TRIzol Reagent™ method with desalting were
388 then applied to answer the question of how *H. salinarum* acclimates to halite brine inclusions over the
389 initial phase post-evaporation using proteomics

390 **4.4 Proteomic Shifts in *H. salinarum* Induced by Acclimation to Halite Brine Inclusions**

391 Total proteins were extracted from the brine inclusions of halite after two months of complete dryness,
392 with surface-bound proteins removed using these new methods detailed above. These brine inclusion
393 extracts were compared to total proteins extracted from *H. salinarum* cultures in stationary growth
394 phase, representing conditions prior to halite formation. The proteins unique to each condition, as well
395 as the common proteome between liquid cultures and from halite interiors were analyzed to determine
396 how *H. salinarum* acclimates to halite brine inclusions.

397 Using mass spectrometry of four replicates from each condition, 1 249 total proteins were
398 identified from stationary phase liquid cultures and 1 052 from halite brine inclusions, representing 1
399 342 unique proteins. Identifications were obtained with high confidence using FDR < 1 % and at least
400 2 unique peptides. Internal comparisons of the four replicate samples per condition revealed a core
401 proteome of 839 proteins common to all sample replicates for liquid cultures and 715 proteins for halite
402 brine inclusion extracts (Figure 4a, b). Of these, 655 proteins were expressed by cells both in liquid
403 cultures and within halite brine inclusions (after referred to "shared proteins"), while 60 specific to
404 halite brine inclusion samples and another 184 only identified from liquid cultures (Figure 4c,
405 Supplementary Table 6-1). KEGG blastKOALA searches provided matches for roughly 75 % of these
406 shared proteins (488 of 655 shared proteins), as well as 62 % of proteins unique to halite brine inclusion
407 samples (37 of 60 proteins) and 52 % of proteins unique to liquid cultures (95 of 184 proteins) (see
408 Supplementary Table 6-2), allowing for functional pathway reconstruction. The halite brine inclusion
409 proteome contained genome maintenance and repair proteins (Nth, UvrB, MutS2) not found expressed
410 by cells from liquid cultures, along with multiple enzymes implicated in amino acid metabolism,
411 metabolism of cofactors, and membrane transport (see Table 2 and Supplementary Table 6-3).

412 A qualitative approach was insufficient to determine differential regulation of protein
413 expression for *H. salinarum* cells within halite brine inclusions. Instead, a quantitative mass
414 spectrometry analysis was also performed. Results from all three injections were pooled to reduce
415 instrument variability (Figure 5). Subsequent 68 proteins from halite brine inclusions were identified
416 with statistically significant changes in expression levels compared to liquid cultures (fold change ≥ 2;
417 see Supplementary Table 6-4 and Supplementary Figure 6-1). KEGG blastKOALA searches provided
418 functional pathway results for 80 % of down-regulated proteins (35 of 44 proteins) and 71 % of up-
419 regulated proteins (17 of 24 proteins) (see Supplementary Table 6-2). Up-regulated proteins included
420 metal transporters, redox reactions, acetyl-CoA production, and the UgpB glycerol-3-phosphate-
421 binding protein precursor. Down-regulated proteins were predominantly ribosomal subunits, indicating

422 reduced translational activity (see Table 2 and Supplementary Table 6-3). To determine whether there
423 was a corresponding downwards shift in transcriptional activity for cells inside halite brine inclusions
424 compared to liquid cultures, RNA extractions were performed.

425 4.5 Reduced Total RNA Concentration Within Halite Brine Inclusions

426 The advantage of a TRIzol Reagent™-based extraction method is that it allows for extraction of not
427 only proteins, but also nucleic acids (DNA, RNA), and lipids (Podechard *et al.,* 2018) for complete
428 multi-omics analyses. To this end, the new methodology presented here was applied to extract and
429 purify RNA from surface cleaned, internally inoculated halite after two months of incubation at 37 ˚C
430 to complement the proteomic analyses. Consistent with the reduced quantities of ribosomal proteins
431 observed for halite brine inclusion extracts, low quantities of RNA were obtained from brine extracts
432 compared to stationary cells extracts (Table 3). In addition, the quality and purity of the resultant RNA
433 from halite was lower than that from liquid cultures (Supplementary Figure 6-2). To determine if this
434 low-quality RNA was due to the age of the samples (two months after drying) or degrading effects of
435 halite salts on RNA during extraction, extractions of RNA were performed from fresh externally
436 inoculated halite (*i.e.*, approximatively one week after external cells addition) using the same protocol.
437 RNA extractions from these 'young' crystals presented higher quantity and purity compared to those
438 from halite brine inclusions after two months, but still lower quality and purity than RNA extracted
439 from liquid cultures.

440 5 Discussion

441 The initial objective of this study was to determine the molecular acclimation of haloarchaea to
442 entrapment within halite brine inclusions using a proteomics approach. To this aim, we first needed to
443 (1) better characterize the process of laboratory-based evaporation for halite entrapment of
444 haloarchaeal and its effects on both the resulting halite and the microbial cells, (2) develop efficient
445 methods for removal of halite surface-bound cells and biomolecules in order to isolate only proteins
446 contained within the brine inclusions, (3) develop effective methods for protein extraction directly from
447 halite brine inclusions in a rapid time period to avoid alterations in protein expression that can occur
448 during gradual salt dissolution, and finally (4) combine these approaches to analyze total proteins and
449 RNA from *H. salinarum* extracted from halite brine inclusions and compare these to control samples
450 from stationary phase liquid cultures in order to propose a model of acclimation within halite. A slow
451 evaporative process was chosen to generate the internally inoculated halite to model natural processes

that occur over time scales sufficient for cellular acclimation to the environmental changes, rather than a rapid "shock" evaporative process.

5.1 Biotic/Abiotic Interactions Influencing Halite Formation and *H. salinarum* Viability

Similar to previous studies of survival of halophiles within halite brine inclusions, a NaCl-based buffered evaporation solution was used in this study (Norton and Grand, 1988; Fendrihan *et al*., 2012; Kixmüller *et al*., 2012). However, here we chose to add nutrient sources (1 % peptone, 0.5 % L-Arg-HCl) to simulate organics present in the natural environment. This enabled us to study the role of metabolism in the survival and acclimation processes of *H. salinarum* cells to the early phases of entrapment within halite brine inclusions. The presence of microbial biomass and additional organics can affect halite precipitation processes and also explain the observed crystallization heterogeneity observed. For example, Norton and Grant (1988) previously demonstrated a positive correlation between the initial microbial cell density in liquid culture and the quantity of halite brine inclusions formed during evaporation.

In addition, the presence of nutrients seemed to diminish rather than increase the duration of survival. While Gramain *et al*. (2011) observed growth of *H. salinarum* NRC-1 after 27 months post-entombed in halite, there were some notable differences in the experimental parameters used. Gramain *et al*. (2011) used evaporation buffers with different compositions of nutrients to the evaporation buffer (either without nutrients or with addition of 0.01 % Difco yeast extract and 0.0075 % Merck casein hydrolysate diluted from the standard concentrations in modified Payne's medium of 1 % and 0.75 %, respectively, Payne *et al.,* 1960), incubated the resulting salt crystals in the dark at RT°C rather than with a 12 h:12 h diurnal cycle at 37 ˚C as used here, and did not appear to employ halite surface sterilization or cleaning protocols prior to these survival tests. In contrast, our viability tests of *H. salinarum* cells from internally inoculated crystals incubated at 37 ˚C over 80 days prior to subjected to surface organics cleaning treatments, dissolution and culturing showed no growth. The lower duration of survival observed for *H. salinarum* cells inside halite in our study may be the result of increased metabolic activity due to the higher concentration of nutrients in TNPA solution (1% peptone) compared to the 100-time diluted modified Payne's medium used in Gramain *et al*. (2011). This could result in an inhibitory effect due to the accumulation of toxic waste products within the closed microenvironment of halite brine inclusions. On the other hand, in the absence of surface sterilization of halite used in the viability studies in Gramain *et al.* (2011), some of the surviving cells observed in the study may have been the result of surface-adhered cells rather than cells within the

halite brine inclusions. These results also suggest a possible survival advantage for cells on halite surfaces rather than those within the brine inclusions over the early stages of evaporation and acclimation, an hypothesis supported by the findings of Gramain *et al.* (2011) showing no difference in growth for *H. salinarum* cells evaporated in salt buffer without nutrients and those containing the diluted Payne's medium nutrients. This epilithic lifestyle stay probable also due to organics observed form surface halite, as well as microscopic sylvite (KCl) crystals derived from the lysis of *H. salinarum* cells were also observed on the surface of the laboratory-grown halite while the vacuum conditions for SEM observations may have resulted in rupture of unfixed cells.

All together, these results of surface contamination confirm that the isolation of proteins exclusively from halite brine requires the removal of halite surface-bound cells and biomolecules.

5.2 Removal of Halite Surface-Bound Microorganisms and Biomolecules

The small sizes of laboratory-grown halite do not allow using treatment processes that could result in salt dissolution. Cold atmospheric plasmas were therefore tested in an effort to avoid the use of liquid cleaners based on their effectiveness for the sterilization of spacecraft surfaces for planetary protection (Shimizu *et al*., 2013) and agricultural applications (Judée *et al*., 2021). Unfortunately, none of the plasma conditions tested in this study (gas mixtures, power delivery modalities) enabled a complete removal of proteins from the rough textured halite surfaces. However, the results remain encouraging insofar as cold plasma has demonstrated effects on proteolysis which must now be amplified. Further experiments will be required to innovate an *ad hoc* plasma process delivering active species at higher densities while treating the whole surface of halites regardless their roughness surface, dimensions or dielectric permittivity.

Therefore, the deactivation of microorganisms and removal of nucleic acids from halite surfaces have been performed by adapting chemical wash methods first developed by Rosenzweig *et al*. (2000) and then optimized by Gramain *et al*. (2011) and Sankaranarayanan *et al*. (2011). By reducing the exposure times in sequential NaOCl, NaOH, and HCl treatments, and replacing passive chemical baths with an active spray process, we were able to achieve sufficient proteolysis of surface-bound proteins for downstream isolation of proteins exclusively from within halite brine inclusions, while avoiding halite dissolution during treatment. Compared to total proteins extracted from surface sterilized internally inoculated crystals (± 1 mg order), residual surface bound proteins (51.6 µg) were marginal. However, observations of residual pigmentation after halite treatment suggest the presence

of non-protein pigments such as carotenoids. Further refinements are therefore needed before future studies can isolate lipids exclusively from within halite brine inclusions.

5.3 Limitations of the TRIzol Reagent™ Based Method for Direct Extraction of Biomolecules From Halite Brine Inclusions

TRIzol Reagent™ has the distinct benefit of enabling selective extraction of proteins, lipids, and nucleic acids. While TRIzol-based protein extraction methods have previously been used and validated to study proteins from liquid cultures of haloarchaea (Kirkland *et al*., 2006; Bidle *et al*., 2008). In this study procedure was modified for direct proteins extraction on salts crystals and subsequent desalinations steps were developed to allow mass spectrometry analysis possible from these high salt extracts. The results obtained after modifications of the procedure by Kirkland *et al*. (2006) procedure appear compatible and efficient for quantitative mass spectrometry approach directly on halite brine inclusions which confirm optimal modifications. In addition, compared to crystal dissolution method prior to proteins extraction, this methodology avoid bias related to dissolution-associated proteome changes.

However, while peripheral membrane proteins were identified, transmembrane peptides were absent from the mass spectrometry dataset. We hypothesize that this was due to retention of transmembrane protein domains with the lipid membrane fraction during TRIzol Reagent™ extraction in residual phenol phase after protein precipitation with isopropanol. Importantly, some transmembrane proteins could be identified by peptides outside the membrane-spanning domains *e.g.*, the ArcD arginine-ornithine antiporter protein, for which seven cytosolic- and extracellular-facing peptides were identified (see Supplementary Figure 7-1). One explanation of this phenomenon is the desalting effect of isopropanol (as suggested by Kirkland *et al*., 2006) that can result in increased protein instability, leading to loss of conformation and subsequent peptide fragmentation for peptides outside the transmembrane regions. While these results indicate that further membrane disruption steps may be needed for complete extraction of all transmembrane proteins, similar to the protocol used by Podechard *et al.,* 2018 to isolate membrane lipids using TRIzol, the potential bias introduced by our methodology is limited, as shown in by the identification of peptides extending to either side of the lipid membrane.

While the low quantities of RNA extracted from halite brine inclusions were likely the result of low transcriptional activity based on the down regulation of ribosomal proteins observed during

proteomics analyses (see following section), it might also be due to the age of the halite with subsequent degradation of RNA after cells trapping. In addition, RNA quantity, purity and quality were insufficient to allow transcriptomics analysis for brine extracts. The quantity, quality and purity scores for fresh externally inoculated crystals were higher than those for surface sterilized crystals incubated for two months. Further desalting steps may help to improve future RNA extraction directly from halite.

5.4 Acclimation of *H. salinarum* to Halite Brine Inclusions

We applied the slow laboratory evaporation method to *H. salinarum* cultures in TNPA buffer followed by removal of halite surface-bound cells and organics (particularly proteins) and selective extraction of proteins from within halite brine inclusions described in the preceding sections. This allowed us to study the early (two month) acclimation of the haloarchaeal cells to halite brine inclusions using a proteomics approach. Stationary growth phase cultures were used as a control to approximate the cell physiology prior to a slow evaporative process. Our analyses were focused on two main themes: (1) cell activity within halite brine inclusions, and (2) interactions between cells and local microenvironment. The investigations of the cell activity targeted proteins involved in central metabolism, energy production, cell division, replication, transcription and translation pathways. The cell interactions with the closed halite brine inclusion microenvironment were examined via cell envelope proteins (surface layer cell wall proteins and transporters) as well as proteins involved in the motility processes (chemotaxis, gas vesicle and archaellum).

5.4.1 Cellular Origin of Total Brine Extracted Proteome

The proteins extracted using the protocol presented here represent the total protein complement of the halite brine inclusion. These proteins may be components of viable or non-viable cells, or even proteins released by cells into the extracellular environment of the brine inclusion. Many questions remain about the potential for salts to preserve proteins over time as molecular biosignatures, particularly within the protected evaporite brine inclusion microenvironment. However, as the *H. salinarum* cells studied here remained viable during the two months of this study, we can hypothesize a cellular origin for the extracted proteins.

5.4.2 Cell Activities Within Halite Brine Inclusions

Table 2 shown similar proteins between cells from the stationary growth stage and brine extracts, suggesting reduced cell division in both conditions. Proteins involved in DNA replication, reparation and transcriptional pathways were shown to be shared without down-regulation, which suppose active

cells or at least few changes comparing late growth stage and brine entombment. However, translational proteins were not detected in brine extracts, suggesting that protein synthesis decrease compared to stationary cells. This surprising result can be explained by a transcriptional activity directed not to mRNA synthesis but to regulatory RNA. However, this hypothesis stays open to criticism, as tRNA synthesis and ribosomal biogenesis proteins remains similar for both conditions.

5.4.3 Halite brine Inclusions Cells Retain Proteins for Central Metabolism

Proteins involved in central metabolism, including key enzymes involved in glycolysis/gluconeogenesis and the TCA cycle, formed part of the shared proteome between halite brine inclusion extracts and stationary phase liquid cultures (Table 2). Additionally, proteins involved in phototrophy, arginine fermentation and aerobic respiration were shared between halite brine inclusions and stationary growth phase liquid cultures. The microenvironment of halite brine inclusions was assumed to be oxygen poor due to the combination of low DO_2 at high salinities as well as the closed microenvironment of brine inclusions. The metabolism of *Halobacterium* cells trapped within such inclusions is therefore hypothesized to shift from aerobic metabolism by respiratory chain to anaerobic fermentation or phototrophy through arginine deiminase pathway (ADI). Incubations of halite were performed with a 12 h:12 h light:dark photoperiod, allowing for phototrophy under oxygen-limited conditions.

Quantitative analyses showed that the majority of proteins involved in pyruvate metabolism maintained consistent expression levels after two months of halite inclusion with the exception of up-regulation of proteins involved in acetyl-CoA production. Surprisingly, transporters and enzymes involved in ADI pathway were expressed by both cells in stationary phase liquid cultures and brine inclusion extracts, including the arginine deiminase, ornithine-carbamoyl transferase, carbamate kinase, arginosuccinase, arginosuccinate synthetase, arginine-ornithine antiporter and an IclR family transcriptional regulator. Only arginine deaminase was found significantly up-regulated for cells from halite brine inclusions. Proteins for key components of the electron transport chain, including NADH dehydrogenase/oxidoreductase subunits B, C, D and I, NAD(P)/FAD-dependent oxidoreductase, succinate dehydrogenases and ATP synthase subunits A, B, C, D, E, H and I were not found to be differentially regulated between cells from free-living (liquid cultures) or trapped within halite brine inclusions (with the exception of with F subunit lacked in one brine inclusion extract). The bacterio-opsin activator-like protein and Htr signal transducer were common to all replicates and conditions, while bacterio-opsin activator was only found in two of the four halite brine inclusion replicate

samples. Confirmation of the precise metabolic pathways used by *H. salinarum* within halite brine inclusions will require further analyses, overcoming the challenges of accessing the closed halite system.

Acclimation to the halite brine inclusions microenvironment could presumably involve reduced or silenced cell division, DNA replication and repair pathways. However, eight proteins involved in chromosome partitioning were found shared between halite brine inclusion extracts and stationary growth phase cultures, along with 11 other proteins involved in DNA replication including matches for DNA primase, polymerase, gyrase, topoisomerase and replication factors. Only four DNA replication proteins were found to be specific to stationary growth phase proteomes. This suggests that either such proteins are constitutively expressed, or that DNA replication and cell division occur in a similar fashion for both stationary growth phase cells and those within halite brine inclusions.

DNA repair processes were represented both within halite brine inclusions and liquid cultures by the DNA photolyase, Rad50, the UvrD repair helicase, UvrA excinuclease, RadA recombinase, Rad25 DNA repair helicase, Fen1 repair endonuclease and the Hel208 helicase are found shared between liquids and brine extracts. Other DNA repair proteins were specific to either halite or liquid samples. Stationary growth phase cultures contained additional repair proteins including the RmeR site-specific deoxyribonuclease, endonuclease IV, RecJ single-strand exonuclease, MutL mismatch repair protein, DNA gyrase and N-glycosylase, whereas the UvrB, MutS and endonuclease III proteins were exclusive to halite brine inclusion proteomes.

Investigations of DNA transcription identified a shared proteome between liquid cultures and brine inclusions including proteins for transcriptional initiation factors (TFIIE and TFIID) and transcriptional machinery (RNA polymerase subunits rpoA2, rpoB1, rpoB2, rpoD and rpoE1). Proteins involved in transfer RNA biogenesis such as tRNA ligases for 18 different amino acids along with two ribonucleases completed the shared transcriptional proteome of liquid cultures cells and halite extracts. Only tRNA ligases specific for tryptophan and threonine, four unique transcriptional proteins (rpoF, rpoH, rpoN and nusA termination protein) and one unique transcription initiation factor (TFIIB) were only found only in stationary growth phase cell extracts.

While early acclimation to the halite brine inclusion microenvironment resulted in nuanced differences in the proteome of *H. salinarum* cells regarding cell division, replication, DNA repair and transcriptional processes, stark differences were observed for proteins involved in translation activities.

634 Translational activities were severely restricted for cell within halite brine inclusions, as evidenced by
635 the down-regulation of 27 of the 42 ribosomal proteins shared by cells from both conditions tested.
636 Only one ribosomal protein was up-regulated. The shared proteome between cells in halite brine
637 inclusions and those in liquid culture included an additional 10 proteins involved in ribosome
638 biogenesis, and 10 translation initiation factors for which non showed any significant up- or down-
639 regulation. Chaperones proteins were showed a high degree of conservation between conditions, with
640 thioredoxin, chaperone DnaJ, DnaK along with the GrPE stimulator, Hsp20, thermosome subunit and
641 prefoldin all shared by both for liquid and halite extracts. Only prefoldin beta subunit was down-
642 regulated for cells from halite brine inclusions.

643 Taken together, these data indicate a high level of similarity between stationary growth phase
644 cells in liquid culture and those trapped within halite brine inclusions. Acclimation to the closed brine
645 inclusion microenvironment appears to severely limit translational activity. However, expressed
646 proteins are preserved indicating low levels of protein turnover. Cells maintain at least the capacity for
647 central metabolism, DNA repair, replication, and even cell division comparable to stationary growth
648 phase cells.

649 **5.4.4 Interactions Between Cells and the Brine Inclusion Microenvironment**

650 the potential interactions between *H. salinarum* cells and the local microenvironment within halite
651 brine inclusions focusing on cell surface and mobility processes involved in responses to external
652 stimuli. Previous investigations of the survival of *Halobacterium* cells trapped within salt crystals have
653 proposed potential for cell envelope modifications with surface proteinaceous layer (S-layer) shed
654 (Fendrihan *et al*., 2012). However, this result seems dependent on conditions (Kixmüller *et al.,* 2012).
655 S-layer shedding thought to improve exchanges between cells and the local microenvironment.
656 However, in this study S-layer proteins were identified in all liquid culture and halite samples without
657 significant up- or down-regulation. This suggests that the S-layer is maintained by *H. salinarum* cells
658 within halite brine inclusions. Additionally, of the 20 membrane transporters shared between the
659 proteomes of liquid cultures and cells inside halite brine inclusions, four were found to be up-regulated
660 in halite brine inclusion extract, including the glycerol-3-phosphate-binding protein precursor.
661 Moreover, six proteins were found to be unique to the halite brine inclusion proteome including
662 phosphate, iron and glycerol-3-phosphate transporters. This suggests that transport capacity is not only
663 maintained but enhanced in cells during acclimation to halite brine inclusions, likely to maximize
664 extraction of essential molecules and trace elements from the local microenvironment.

Previous published transcriptomics and proteomics studies on *H. salinarum* cell shown impact of salinity and dissolved oxygen concentrations on motility (Schmid *et al*., 2007; Leuko *et al*., 2009). We therefore examined the expression of archaellum, gas vesicles and chemotaxis proteins. A high degree of variability was noted in the expression of these proteins between halite brine inclusion extracts and stationary growth phase cultures. Some proteins were common to both proteomes without any differences in protein quantities, including for the gas vesicle protein (Gvp) subunits F, C, N of cluster A, while GvpA was found only in two of the four liquid cultures and two of four halite samples. GvpD and I subunits of A cluster and F of B cluster were found punctually in liquid samples. Only GvpO cluster A and B seems to be impacted by crystallization with significant down-regulation in halite brine inclusion extracts. For the archaellum proteins, only archaellin B1 was down-regulated in halite samples whereas achaellin A1 and prearchaellin peptidase were identified punctually in liquid culture samples. Archaellin B2, A2 and flagellin related H protein were found in all liquid culture replicates but only in one halite replicate. An examination of chemotaxis proteins showed that all 18 identified proteins including CheR, CheA, CheW, CheC, CheB and mcp family proteins were shared between halite brine inclusions extract and stationary growth phase liquid cultures.

These data show a general down-regulation of archaellin proteins involved in motility. A reduced motility may be induced in halite brine inclusions to preserve energy. Gas vesicle down-regulation suggests a lack of needed capacity for vertical movement in a water column in response to oxygen levels, consistent with the restricted confines of a microscopic halite brine inclusions. Although no swim or floating occur for brine inclusions, cells remain able to receive environmental signals due to chemotaxis proteins founded both in stationary cells and brine extract without significant differential expression.

6 Conclusion

The methods presented in this study expand on previous protocols for deactivation of halite surface-attached cells removal of nucleic acids and allow for the first time for isolation of proteins directly from halite brine inclusions that both excludes surface-bound contaminating proteins and avoids changes in cell protein expression during salt dissolution. These methodologies were applied here to provide the first sights into the molecular mechanisms involved in early acclamation of *H. salinarum* within brine inclusions. While further functional investigations are needed to confirm the proteomics hypotheses generated by the data in this study, the methodologies presented here could also have future applications for the study of microorganisms in halite inclusions in natural settings.

7 Data Availability Statement

Proteomics data are available to the ProteomeXchange Consortium via the PRIDE partner repository with the dataset identifier (*under submission*).

8 Author Contributions

Study was designed by CF, AK, AH and SZ under supervision of AK, SZ and AH. Experiments were conducted by CF with the help of MM for crystals forming; AM and RP for mass spectrometry and improvements of extraction methods; BAB for nanoLC-MS/MS data acquisition; FG for MEB-EDX analyses; AT for RNA extraction and TD for plasma treatments. Proteomics data treatments were conducted by AT and CF. Manuscript was written by CF and then revised and approved by all co-authors.

9 Acknowledgments

This work was supported by Sorbonne Université, the X-life program of CNRS-MITI, the ATM program of the Muséum National d'Histoire Naturelle and the ANR program "ExocubeHALO" (ANR-21-CE49-0017-01_ACT). The UHPLC MS/MS data were acquired at the Plateau technique de spectrométrie de masse bio-organique, UMR 7245 Molécules de Communication et d'Adaptation des Microorganismes, Muséum national d'Histoire naturelle, Paris, France. The nanoLC-MS/MS data were acquired at ProGenoMix MS-platform at CEA-Marcoule. The SEM-EDX images were acquired at the Plateforme de microscopie électronique from IMPMC. Parts of the figure were drawn by using pictures from Servier Medical Art. Servier Medical Art by Servier is licensed under a Creative Commons Attribution 3.0 Unported License (https://creativecommons.org/licenses/by/3.0/).

10 Supplementary

The supplementary for this article are available online.

11 References

Bidle, K. A., Kirkland, P. A., Nannen, J. L., and Maupin-Furlow, J. A. (2008). Proteomic analysis of *Haloferax volcanii* reveals salinity-mediated regulation of the stress response protein PspA. Microbiol Read Engl 154, 1436–43. doi: 10.1099/mic.0.2007/015586-0.

Coker, J. A., DasSarma, P., Kumar, J., Müller, J. A., and DasSarma, S. (2007). Transcriptional profiling of the model Archaeon *Halobacterium* sp. NRC-1: responses to changes in salinity and temperature. Saline Syst 3, 6. doi: 10.1186/1746-1448-3-6.

Engel, M. B., and Catchpole, H. R. (2005). A microprobe analysis of inorganic elements in *Halobacterium salinarum*. Cell Biol Int 29, 616–622. doi: 10.1016/j.cellbi.2005.03.024.

Falb, M., Müller, K., Königsmaier, L., Oberwinkler, T., Horn, P., Gronau, S. von, et al. (2008). Metabolism of halophilic archaea. Extremophiles 12, 177–196. doi: 10.1007/s00792-008-0138-x.

Fendrihan, S., Dornmayr-Pfaffenhuemer, M., Gerbl, F. W., Holzinger, A., Grösbacher, M., Briza, P., et al. (2012). Spherical particles of halophilic archaea correlate with exposure to low water activity – implications for microbial survival in fluid inclusions of ancient halite. Geobiology 10, 424–433. doi: 10.1111/j.1472-4669.2012.00337.x.

Gonzalez, O., Gronau, S., Pfeiffer, F., Mendoza, E., Zimmer, R., and Oesterhelt, D. (2009). Systems Analysis of Bioenergetics and Growth of the Extreme Halophile *Halobacterium salinarum*. Plos Comput Biol 5, e1000332. doi: 10.1371/journal.pcbi.1000332.

Gramain, A., Díaz, G. C., Demergasso, C., Lowenstein, T. K., and McGenity, T. J. (2011). Archaeal diversity along a subterranean salt core from the Salar Grande (Chile). Environ Microbiol 13, 2105–2121. doi: 10.1111/j.1462-2920.2011.02435.x.

Graur, D., and Pupko, T. (2001). The Permian Bacterium that Isn't.

Gruber, C., Legat, A., Pfaffenhuemer, M., Radax, C., Weidler, G., Busse, H.-J., et al. (2004). *Halobacterium noricense* sp. nov., an archaeal isolate from a bore core of an alpine Permian salt deposit, classification of *Halobacterium* sp. NRC-1 as a strain of *H. salinarum* and emended description of *H. salinarum*. Extremophiles 8, 431–439. doi: 10.1007/s00792-004-0403-6.

Hartmann, R., Sickinger, H. D., and Oesterhelt, D. (1980). Anaerobic growth of halobacteria. Proc National Acad Sci 77, 3821–3825. doi: 10.1073/pnas.77.7.3821.

Huby, T. J. C., Clark, D. R., McKew, B. A., and McGenity, T. J. (2020). Extremely halophilic archaeal communities are resilient to short-term entombment in halite. Environ Microbiol. doi: 10.1111/1462-2920.14913.

Judée, F., Simon, S., Bailly, C., and Dufour, T. (2018). Plasma-activation of tap water using DBD for agronomy applications: Identification and quantification of long lifetime chemical species and production/consumption mechanisms. Water Res 133, 47–59. doi: 10.1016/j.watres.2017.12.035.

Kanehisa, M., and Goto, S. (2000). KEGG: Kyoto Encyclopedia of Genes and Genomes. Nucleic Acids Res 28, 27–30. doi: 10.1093/nar/28.1.27.

Kanehisa, M., Sato, Y., and Morishima, K. (2016). BlastKOALA and GhostKOALA: KEGG Tools for Functional Characterization of Genome and Metagenome Sequences. J Mol Biol 428, 726–731. doi: 10.1016/j.jmb.2015.11.006.

Kirkland, P. A., Busby, J., Stevens, S., and Maupin-Furlow, J. A. (2006). Trizol-based method for sample preparation and isoelectric focusing of halophilic proteins. Anal Biochem 351, 254–259. doi: 10.1016/j.ab.2006.01.017.

Kixmüller, D., and Greie, J. (2012). An ATP-driven potassium pump promotes long-term survival of Halobacterium salinarum within salt crystals. Env Microbiol Rep 4, 234–241. doi: 10.1111/j.1758-2229.2012.00326.x.

Leuko, S., Raftery, M. J., Burns, B. P., Walter, M. R., and Neilan, B. A. (2009). Global Protein-Level Responses of *Halobacterium salinarum* NRC-1 to Prolonged Changes in External Sodium Chloride Concentrations. J Proteome Res 8, 2218–2225. doi: 10.1021/pr800663c.

Maughan, H., Birky, W., Nicholson, W., Rosenzweig, W., and Vreeland, R. (2002). The paradox of the "ancient" bacterium rich contains "modern" protein-coding genes.

Merino, N., Aronson, H. S., Bojanova, D. P., Feyhl-Buska, J., Wong, M. L., Zhang, S., et al. (2019). Living at the Extremes: Extremophiles and the Limits of Life in a Planetary Context. Front Microbiol 10, 780. doi: 10.3389/fmicb.2019.00780.

Moran-Reyna, A., and Coker, J. A. (2014). The effects of extremes of pH on the growth and transcriptomic profiles of three haloarchaea. F1000research3, 168. doi: 10.12688/f1000research.4789.2.

Mormile, M. R., Biesen, M. A., Gutierrez, M. C., Ventosa, A., Pavlovich, J. B., Onstott, T. C., et al. (2003). Isolation of *Halobacterium salinarum* retrieved directly from halite brine inclusions. Environ Microbiol 5, 1094–1102. doi: 10.1046/j.1462-2920.2003.00509.x.

Müller, J. A., and DasSarma, S. (2005). Genomic Analysis of Anaerobic Respiration in the Archaeon *Halobacterium* sp. Strain NRC-1: Dimethyl Sulfoxide and Trimethylamine N-Oxide as Terminal Electron Acceptors. J Bacteriol 187, 1659–1667. doi: 10.1128/jb.187.5.1659-1667.2005.

Nickle, D. C., Learn, G. H., Rain, M. W., Mullins, J. I., and Mittler, J. E. (2002). Curiously Modern DNA for a "250 Million-Year-Old" Bacterium. J Mol Evol 54, 134–137. doi: 10.1007/s00239-001-0025-x.

Nims, C., Lafond, J., Alleon, J., Templeton, A. S., and Cosmidis, J. (2021). Organic biomorphs may be better preserved than microorganisms in early Earth sediments. Geology 49, 629–634. doi: 10.1130/g48152.1.

Norton, C. F., and Grant, W. D. (1988). Survival of Halobacteria Within Fluid Inclusions in Salt Crystals. Journal of General Microbiology, 1365–1373.

Oesterhelt, D., and Stoeckenius, W. (1974). Methods in Enzymology. Methods Enzymol 31, 667–678. doi: 10.1016/0076-6879(74)31072-5.

Oren, A., Arahal, D. R., and Ventosa, A. (2009). Emended descriptions of genera of the family Halobacteriaceae. Int J Syst Evol Micr 59, 637–642. doi: 10.1099/ijs.0.008904-0.

Oren, A. (2006). Life at high salt concentrations. The prokaryotes 3, 263–282. doi: 10.1007/0-387-30742-7-9.

Payne, J. I., Sehgal, S. N., and Gibbons, N. E. (1960). Immersion Refractometry of some halophilic bacteria. Can J Microbiol 6, 9–15. doi: 10.1139/m60-002.

Pinel-Cabello, M., Chapon, V., Ruiz-Fresneda, M. A., Alpha-Bazin, B., Berthomieu, C., Armengaud, J., et al. (2021). Delineation of cellular stages and identification of key proteins for reduction and biotransformation of Se(IV) by Stenotrophomonas bentonitica BII-R7. J Hazard Mater 418, 126150. doi: 10.1016/j.jhazmat.2021.126150.

Podechard, N., Ducheix, S., Polizzi, A., Lasserre, F., Montagner, A., Legagneux, V., et al. (2018). Dual extraction of mRNA and lipids from a single biological sample. Sci Rep-uk 8, 7019. doi: 10.1038/s41598-018-25332-9.

Post, F. J. (1977). The microbial ecology of the Great Salt Lake. Microbial Ecol 3, 143–165. doi: 10.1007/bf02010403.

Roedder, E. (1984). The fluids in salt. American Mineralogist 69, 413–439.

Rosenzweig, W. D., Peterson, J., Woish, J., and Vreeland, R. H. (2000). Development of a Protocol to Retrieve Microorganisms from Ancient Salt Crystals. Geomicrobiol J 17, 185–192. doi: 10.1080/01490450050121152.

Sankaranarayanan, K., Timofeeff, M. N., Spathis, R., Lowenstein, T. K., and Lum, J. K. (2011). Ancient Microbes from Halite Fluid Inclusions: Optimized Surface Sterilization and DNA Extraction. Plos One 6, e20683. doi: 10.1371/journal.pone.0020683.

Schmid, A. K., Reiss, D. J., Pan, M., Koide, T., and Baliga, N. S. (2009). A single transcription factor regulates evolutionarily diverse but functionally linked metabolic pathways in response to nutrient availability. Mol Syst Biol 5, 282. doi: 10.1038/msb.2009.40.

Schreder-Gomes, S. I., Benison, K. C., and Bernau, J. A. (2022). 830-million-year-old microorganisms in primary fluid inclusions in halite. Geology. doi: 10.1130/g49957.1.

Shimizu, S., Barczyk, S., Rettberg, P., Shimizu, T., Klaempfl, T., Zimmermann, J. L., et al. (2014). Cold atmospheric plasma – A new technology for spacecraft component decontamination. Planet Space Sci 90, 60–71. doi: 10.1016/j.pss.2013.10.008.

Tebbe, A., Schmidt, A., Konstantinidis, K., Falb, M., Bisle, B., Klein, C., et al. (2009). Life-style changes of a halophilic archaeon analyzed by quantitative proteomics. Proteomics 9, 3843–3855. doi: 10.1002/pmic.200800944.

Vreeland, R. H., Rosenzweig, W. D., and Powers, D. W. (2000). Isolation of a 250 million-year-old halotolerant bacterium from a primary salt crystal. Nature 407, 897–900. doi: 10.1038/35038060.

Winters, Y. D., Lowenstein, T. K., and Timofeeff, M. N. (2015). Starvation-Survival in Haloarchaea. Life 5, 1587–1609. doi: 10.3390/life5041587.

12 Table and Figures

Table 1: Experimental parameters of cold plasma sources used to remove surface-bound proteins. The evaluation is based of proteolysis results. DBD means dielectric barrier device; APPJ for atmospheric pressure plasma jet. Slm stands for standard liters per minute and sccm standard centimeters cube per minute.

Plasma source	Excitation mode	Electrical parameters			Gas and flow rate	Proteolysis
		Ampl.	Freq.	Duty cycle		
DBD	Alternative Current	7 kV	500 Hz	-	He (1 slm)	0.0 %
					He-O_2 (1slm - 150 sccm)	0.0 %
					He-O_2 (1slm - 3 sccm)	0.0 %
					Ar (1 slm)	0.0 %
APPJ	Alternative Current	7 kV	700 Hz	-	He (6 slm)	0.0 %
	Pulse	7 kV	700 Hz	1 %	He (6 slm)	29.3 %
					He-O_2 (6 slm - 100 sccm)	39.1 %

Table 2: Targeted proteins involved in early acclimation of *Halobacterium salinarum* through halite brine inclusion (for extended matched proteins, see Supplementary Table 6-5). Shared mean protein found for all the fourth brine extract and the fourth liquids stationary extracts.

Central metabolism - glycolysis/gluconeogenesis		**Samples**
AAG20336.1	phosphohexomutase (phosphoglucomutase /phosphomannomutase)	Shared
AAG20164.1	glucose-6-phosphate isomerase	Shared
AAG19177.1	fructose-bisphosphatase	Shared
AAG19176.1	class I fructose-bisphosphate aldolase	Shared
AAG19439.1	triosephosphate isomerase	Shared
AAG18725.1	glyceraldehyde 3-phosphate dehydrogenase	Shared
AAG19584.1	phosphoglycerate kinase <-> glucose-6-phosphate isomerase	Shared
AAG20083.1	phosphoglycerate mutase	Shared
AAG19526.1	phosphopyruvate hydratase	Shared
AAG18902.1	pyruvate kinase	Shared
AAG18906.1	phosphoenolpyruvate synthase	Shared
Central metabolism - tricarboxylic acid (TCA) cycle		
AAG20246.1	citrate synthase	Shared
AAG20620.1	aconitase	Shared
AAG20073.1	isocitrate dehydrogenase NADP	Shared
DAC78228.1	pyruvate--ferredoxin oxidoreductase alphasubunit	Shared
AAG19513.1	2-ketoglutarate ferredoxin oxidoreductase	Shared
AAG19826.1	succinyl-CoA synthetase beta chain	Shared
AAG19827.1	succinyl-CoA synthetase alpha chain	Shared
AAG19651.1	succinate dehydrogenase subunit A	Shared
AAG19652.1	succinate dehydrogenase subunit B	Shared
AAG19688.1	fumarate hydratase	Shared
AAG20463.1	L-malate dehydrogenase	Shared
Central metabolism - acetyl-CoA metabolism		
AAG19414.1	acetyl-CoA synthetase	Shared
AAG19020.1	acetyl-CoA synthetase	Shared
DAC78075.1	acetate--CoA ligase	Shared
AAG19243.1	aldehyde dehydrogenase (retinol)	Shared
Arginine deiminase pathway		
AAG20948.1	arginine deiminase (plasmid)	Up-regulated
AAG20946.1	ornithine carbamoyltransferase (plasmid)	Shared
AAG20947.1	carbamate kinase (plasmid)	Shared
AAG20518.1	argininosuccinate lyase	Shared
AAG20519.1	argininosuccinate synthetase	Shared
AAG20945.1	Arginine/ornithine antiporter ArcD	Shared
AAG20949.1	lcIR family transcription regulator ArcR (plasmid)	Shared
Aerobic respiration		
AAG19138.1	NADH dehydrogenase/oxidoreductase	Shared
AAG19139.1	NADH dehydrogenase/oxidoreductase	Shared
AAG19141.1	NADH dehydrogenase/oxidoreductase-like protein	Shared
AAG19331.1	NADH dehydrogenase	Shared
AAG19651.1	succinate dehydrogenase subunit A	Shared
AAG19652.1	succinate dehydrogenase subunit B	Shared
AAG20249.1	succinate dehydrogenase subunit	Shared
AAG20277.1	H+-transporting ATP synthase subunit A	Shared
AAG20276.1	H+-transporting ATP synthase subunit B	Shared
AAG20279.1	H+-transporting ATP synthase subunit C	Shared
AAG20273.1	H+-transporting ATP synthase subunit D	Shared
AAG20280.1	H+-transporting ATP synthase subunit E	Shared
AAG20283.1	ATP synthase archaeal subunit H	Shared
AAG20282.1	H+-transporting ATP synthase subunit I	Shared
AAG20278.1	H+-transporting ATP synthase subunit F	Lacked in brine inclusion 4
Bacteriorhodopsin-mediated phototrophy		
AAG18778.1	bacterio-opsin activator-like protein	Shared
AAG19769.1	bacterio-opsin activator	Specific brine inclusion 1, 4
AAG19913.1	sensory rhodopsin I transducer; Htr1 transducer	Shared
AAG19989.1	sensory rhodopsin II transducer; Htr2 transducer	Shared
Cell division and chromosome partitioning associated		
AAG20773.1	chromosome partitioning protein ParA	Shared
AAG18937.1	cell division protein FtsZ type I	Shared
AAG18804.1	cell division protein FtsZ type II	Shared
AAG19919.1	Cell division cycle protein; AAA-type ATPase (CDC48 subfamily)	Shared
AAG19776.1	Cell division cycle protein; AAA-type ATPase (CDC48 subfamily)	Shared
AAG19516.1	Mrp protein homolog	Shared
AAG20269.1	cell division inhibitor MinD/ParA family protein	Shared
AAG20524.1	DNA starvation/stationary phase protection protein; ferritin DspA	Shared
AAG18755.1	archaeal histone A1	Shared
AAG20951.1	chromosome segregation protein SMC	Shared
DNA replication and repair		
AAG19883.1	replication factor C large subunit	Shared
AAG20394.1	replication factor C small subunit	Shared
AAG20005.1	DNA primase DnaG	Shared
AAG19049.1	DNA-directed DNA polymerase B	Shared
AAG19329.1	DNA gyrase subunit A	Shared
AAG19326.1	DNA topoisomerase VI subunit A	Shared
AAG19327.1	DNA topoisomerase VI subunit B	Shared
DAC77610.1	DNA topoisomerase I	Shared
AAG20376.1	DNA polymerase sliding clamp	Shared
AAG20387.1	Orc1-type DNA replication protein	Shared
AAG19323.1	ATP-dependent DNA ligase	Shared
AAG19328.1	DNA gyrase subunit B	Lacked in brine inclusion 4
AAG18851.1	ribonuclease H type 1	All stationary and brine inclusion 2
AAG20362.1	replication factor C small subunit	Lacked in brine inclusion 1
AAG20498.1	Orc1-type DNA replication protein	All stationary and brine inclusion 1
AAG19899.1	ribonucleoside reductase large chain	Shared
AAG19981.1	DNA photolyase family protein	Shared
AAG19671.1	DNA photolyase family protein	Shared
AAG19045.1	DNA double-strand break repair Rad50 ATPase	Shared
AAG20657.1	repair helicase UvrD	Shared
AAG20669.1	excinuclease ABC subunit UvrA	Shared
AAG20465.1	ATP-dependent DNA helicase Hel308	Shared
DAC79307.1	DNA repair and recombination protein RadA	Shared
AAG19690.1	DNA repair protein; flap endonuclease Fen1	Shared
DAC78445.1	DNA repair helicase Rad25	Shared
AAG20482.1	excinuclease ABC subunit UvrB	Lacked in stationary extract 3
AAG20386.1	DNA mismatch repair protein MutS	Lacked in stationary extract 2
AAG19103.1	endonuclease III	Lacked in stationary extract 1
AAG20477.1	type I site-specific deoxyribonuclease subunit RmeR	All stationary and brine extract 1, 3
AAG18797.1	endonuclease IV	All stationary extract
AAG19328.1	DNA gyrase subunit B	Lacked in brine inclusion 4
AAG18777.1	DNA mismatch repair protein MutL	Lacked in brine inclusion 1
AAG19622.1	DNA N-glycosylase	Lacked in brine inclusion 2
AAG20439.1	single-stranded-DNA-specific exonuclease RecJ1	Lacked in brine inclusion 2
Transcriptionnal machinery and factors		
AAG20691.1	DNA-directed RNA polymerase subunit C	Shared
AAG20693.1	DNA-directed RNA polymerase subunit B'	Shared
AAG20694.1	DNA-directed RNA polymerase subunit B"	Shared
AAG19520.1	DNA-directed RNA polymerase subunit D	Shared
AAG20209.1	DNA-directed RNA polymerase subunit E'	Shared
AAG20743.1	transcription initiation factor IID (plasmid); TATA-box-binding protein B	Shared
AAG20365.1	transcription initiation factor IID; TATA-box-binding protein E	Shared
DAC77935.1	transcription initiation factor TFE alpha subunit	Shared
AAG20690.1	NusA-like transcription termination signal-binding factor	Lacked in brine inclusion 4
AAG19546.1	DNA-directed RNA polymerase subunit F	Shared
AAG20695.1	DNA-directed RNA polymerase subunit H	Down-regulated
AAG19524.1	DNA-directed RNA polymerase subunit N	All stationary extracts
AAG18850.1	transcription initiation factor IIB	Lacked in brine inclusion 1
Transfert RNA biogenesis		
AAG20361.1	ribonuclease Z	Shared
AAG20359.1	tyrosine-tRNA ligase	Shared
AAG20355.1	tryptophanyl-tRNA ligase	Shared
AAG20349.1	leucine-tRNA ligase	Shared
AAG20324.1	isoleucine-tRNA ligase	Shared
AAG20397.1	alanine-tRNA ligase	Shared
AAG20602.1	Valine-tRNA ligase	Shared
AAG18903.1	methionine-tRNA ligase	Shared
AAG20222.1	serine-tRNA ligase	Shared
AAG20454.1	glycine-tRNA ligase	Shared
DAC77651.1	proline-tRNA ligase	Shared
AAG19494.1	cysteine-tRNA ligase	Shared
AAG19534.1	glutamate-tRNA ligase	Shared
AAG20944.1	arginine-tRNA ligase	Shared
AAG20567.1	phenylalanine-tRNA ligase alpha chain	Shared
AAG20568.1	phenylalanine-tRNA ligase beta chain	Shared
AAG20175.1	histidine-tRNA ligase	Shared
AAG20183.1	lysine-tRNA ligase	Shared
AAG19001.1	nondiscriminating Aspartyl – tRNA(Asp/Asn) ligase	Shared
AAG20252.1	tRNA(Ile2) 2-agmatinylcytidine synthetase TiaS	Shared
AAG18757.1	tRNA adenylyltransferase CCA-adding	Shared
AAG20422.1	L-threonylcarbamoyladenylate synthase	Shared
AAG20156.1	tRNA pseudouridine synthase Pus10	Shared
AAG20680.1	ribonuclease R	Shared
AAG19760.1	tRNA-splicing ligase RtcB	Shared
AAG19031.1	tRNA/rRNA cytosine-C5-methylase	Shared
AAG20338.1	tryptophan-tRNA ligase	All stationary extracts
AAG20043.1	threonine-tRNA ligase	All stationary extracts
AAG20339.1	tRNA-intron endonuclease	All stationary extracts
AAG19436.1	PtpS family protein	All stationary extracts
AAG18973.1	L-isoaspartyl protein carboxyl methyltransferase	All stationary extracts
AAG20139.1	archaeosine tRNA-ribosyltransferase	All stationary extracts

Ribosome biogenesis		
AAG20650.1	ribosome biogenesis/translation initiation ATPase RLI	Shared
AAG20352.1	probable ribosome biogenesis protein Dim2	Shared
AAG19629.1	ribosome maturation protein Sdo1	Shared
DAC78346.1	ribosome-associating GTPase HflX	Shared
AAG19036.1	GTP-binding protein	Shared
AAG19552.1	fibrillarin-like rRNA/tRNA 2'-O-methyltransferase	Shared
AAG19551.1	rRNA/tRNA 2'-O-methyltransferase complex proteinNop5	Shared
AAG20422.1	L-threonylcarbamoyladenylate synthase	Shared
AAG19112.1	ribonucleoside-diphosphate reductase beta subunit	Shared
AAG20662.1	probable ribonuclease FAU-1	Shared
Translational machinery and factors		
AAG19500.1	50S ribosomal protein L1P	Shared
AAG19501.1	50S ribosomal protein L11P	Shared
AAG19946.1	50S ribosomal protein L14P	Shared
AAG18792.1	50S ribosomal protein L15E	Shared
AAG19941.1	50S ribosomal protein L22P	Shared
AAG19938.1	50S ribosomal protein L23P	Shared
AAG19943.1	50S ribosomal protein L29P	Shared
AAG19936.1	50S ribosomal protein L13P	Shared
AAG19952.1	50S ribosomal protein L6P	Shared
AAG20681.1	30S ribosomal protein S10P	Shared
AAG19256.1	30S ribosomal protein S15P	Shared
AAG19945.1	30S ribosomal protein S17P	Shared
AAG20178.1	30S ribosomal protein S19E	Shared
AAG20206.1	30S ribosomal protein S24E	Shared
AAG19942.1	30S ribosomal protein S3P	Shared
AAG19253.1	30S ribosomal protein S3E	Shared
AAG19556.1	30S ribosomal protein S5P	Shared
AAG20576.1	30S ribosomal protein S6E	Shared
AAG20688.1	30S ribosomal protein S7P	Shared
AAG19951.1	30S ribosomal protein S8P	Shared
AAG19499.1	50S ribosomal protein L10P	Down-regulated
AAG18728.1	50S ribosomal protein L10E	Down-regulated
AAG19522.1	50S ribosomal protein L13P	Down-regulated
AAG19521.1	50S ribosomal protein L18E	Down-regulated
AAG19954.1	50S ribosomal protein L19E	Down-regulated
AAG19939.1	50S ribosomal protein L2P	Down-regulated
AAG19947.1	50S ribosomal protein L24P	Down-regulated
AAG19957.1	50S ribosomal protein L30P	Down-regulated
AAG19953.1	50S ribosomal protein L32E	Down-regulated
AAG19937.1	50S ribosomal protein L4E	Down-regulated
AAG19949.1	50S ribosomal protein L5P	Down-regulated
AAG19537.1	50S ribosomal protein L7Ae	Down-regulated
AAG19519.1	30S ribosomal protein S11P	Down-regulated
AAG20689.1	30S ribosomal protein S12P	Down-regulated
AAG19517.1	30S ribosomal protein S13P	Down-regulated
AAG19950.1	30S ribosomal protein S14P	Down-regulated
AAG19940.1	30S ribosomal protein S19P	Down-regulated
AAG19527.1	30S ribosomal protein S2P	Down-regulated
AAG19518.1	30S ribosomal protein S4P	Down-regulated
AAG19948.1	30S ribosomal protein S4E	Down-regulated
AAG19920.1	30S ribosomal protein S8E	Down-regulated
DAC78237.1	30S ribosomal protein S9	Down-regulated
AAG19070.1	translation initiation factor eIF-2 subunit alpha	Shared
AAG19619.1	translation initiation factor eIF-2 subunit beta	Shared
AAG20211.1	translation initiation factor eIF-2 subunit gamma	Shared
AAG19992.1	translation initiation factor eIF-5A	Shared
AAG19758.1	translation initiation factor eIF-2B subunit delta	Shared
AAG20682.1	translation elongation factor eEF-1A subunit alpha	Shared
AAG19926.1	homolog to translation elongation factor aEF-1alpha subunit	Shared
DAC79456.1	translation elongation factor aEF-2	Shared
AAG20628.1	translation initiation factor aIF-1	Down-regulated
AAG20168.1	translation initiation factor aIF-5B	Up-regulated
Chaperonnes and folding catalysts		
AAG20641.1	thioredoxin	Shared
AAG19025.1	molecular chaperone DnaJ	Shared
AAG19026.1	Hsp70-type molecular chaperone DnaK	Shared
AAG19028.1	DnaJ/DnaK ATPase stimulator GrpE	Shared
AAG19995.1	Hsp20-type molecular chaperone	Shared
AAG18869.1	Hsp20-type molecular chaperone	Shared
AAG20240.1	thermosome subunit beta	Shared
AAG20539.1	prefoldin alpha subunit	Shared
AAG18836.1	prefoldin subunit beta	Down-regulated
Surface proteinaceous layer		
AAG20702.1	cell surface glycoprotein	Shared
Transporters		
AAG18929.1	arsenical pump-driving ATPase ArsA	Shared
AAG19127.1	propionyl-CoA carboxylase carboxyltransferasecomponent	Shared
AAG20473.1	copper transport ATP-binding protein	Shared
AAG19180.1	ABC transporter ATP-binding protein	Shared
AAG19353.1	spermidine/putrescine ABC transporter ATP-binding	Shared
AAG20071.1	spermidine/putrescine ABC transporter	Shared
AAG20612.1	ABC-type transport system periplasmic substrate-binding protein	Shared
AAG20603.1	ABC-type transport system periplasmic substrate-binding protein	Shared
AAG20587.1	dipeptide ABC transporter ATP-binding	Shared
AAG20588.1	dipeptide ABC transporter ATP-binding	Shared
AAG20452.1	dipeptide ABC transporter dipeptide-binding	Shared
AAG20449.1	oligopeptide ABC transporter	Shared
AAG20448.1	oligopeptide ABC transporter ATP-binding	Shared
AAG20457.1	oligopeptide binding protein	Shared
AAG18995.1	phosphate import ATP-binding protein PstB 1	Shared
AAG20556.1	phosphate ABC transporter binding	Shared
AAG18998.1	phosphate ABC transporter substrate-binding protein PstS family	Shared
AAG20233.1	phosphate/phosphite/phosphonate ABC transporter substrate-binding protein	Shared
AAG20486.1	thiamine ABC transporter substrate-binding protein	Shared
AAG20882.1	TrkA family potassium uptake protein	Shared
AAG20878.1	TrkA family potassium uptake protein	Shared
DAC78851.1	TrkA family potassium uptake protein	Shared
AAG20419.1	hemolysin family protein	Shared
AAG19086.1	Mrp-type sodium/proton antiporter system subunit	Shared
AAG18746.1	ABC-type transport system ATP-binding/permease protein	Shared
AAG19338.1	BMP family protein	Shared
DAC77962.1	chemotactic signal transduction system periplasmic substrate-binding protein; BMP family protein	Shared
AAG19051.1	Fe-S cluster assembly ATPase SufC	Shared
AAG20945.1	arginine/ornithine antiporter ArcD	Shared
DAC77887.1	ABC-type transport system permease protein	Lacked in stationary 2, 3
AAG19355.1	iron ABC transporter substrate-binding protein	All brine inclusion
AAG20553.1	phosphate import ATP-binding protein PstB 2	All brine inclusion
AAG20937.1	hemolysin family protein	All brine inclusion
AAG20918.1	glycerol-3-phosphate-binding protein precursor (plasmid)	All brine inclusion
AAG20070.1	PotD/PodF family extracellular solute-binding protein	All brine inclusion
AAG19271.1	spermidine/putrescine-binding protein	All brine inclusion
AAG20451.1	ABC transporter permease	All stationary extracts
AAG20450.1	dipeptide ABC transporter permease	All stationary extracts
AAG19633.1	TrkA family potassium uptake protein	All stationary extracts
AAG18790.1	TrkA family potassium uptake protein	All stationary extracts
AAG19697.1	iron (III) ABC transporter ATP-binding / VitB12-binding protein precursor	All stationary extracts
Archaellum proteins		
AAG19424.1	flagellin A1 precursor	Stationary extracts 1, 2
AAG19384.1	flagellin B2 precursor	Lacked in brine inclusion 1, 2, 4
AAG19383.1	flagellin B1 precursor	Down-regulated
AAG19425.1	flagellin A2 precursor	Lacked in brine inclusion 1, 2, 3
AAG19380.1	flagella-related protein E	Shared
AAG19377.1	flagella-related protein H	Stationary extract 3; brine inclusions 3, 4
DAC79152.1	preplin/prearchaellin peptidase	Stationary extratcs 1, 3, 4
Gas vesicle proteins		
AAG20723.1	Gas vesicle protein GvpF cluster A (plasmid)	Shared
AAG20727.1	Gas vesicle protein GvpC cluster A (plasmid)	Shared
AAG20898.1	Gas vesicle protein GvpO cluster A (plasmid)	Down-regulated
AAG20729.1	Gas vesicle protein GvpO cluster B (plasmid)	Down-regulated
AAG20721.1	Gas vesicle protein GvpH cluster A (plasmid)	All stationary extracts
AAG20728.1	Gas vesicle protein GvpN cluster A (plasmid)	Shared
AAG20717.1	Gas vesicle protein GvpL cluster A (plasmid)	Stationary extracts 1, 2, 4
AAG20725.1	Gas vesicle protein GvpD cluster A (plasmid)	Stationary extract 1
AAG20726.1	Gas vesicle protein GvpA cluster A (plasmid)	Stationary extract 2, 3; brine inclusions 1, 2
AAG20720.1	Gas vesicle protein GvpI cluster A (plasmid)	Stationary extract 2
AAG20892.1	Gas vesicle protein GvpF cluster B (plasmid)	Stationary extract 3, 4
Chemotaxis proteins		
AAG19389.1	chemotaxis protein, protein-glutamate O-methyltransferase CheR	Shared
AAG19394.1	chemotaxis protein, protein-glutamate methylesterase /protein-glutamine glutaminase CheB	Shared
AAG19393.1	taxis sensor histidine kinase CheA	Shared
AAG19396.1	purine-binding taxis protein CheW	Shared
AAG19371.1	purine-binding taxis protein CheW	Shared
AAG19392.1	chemotaxis protein CheC	Shared
AAG19391.1	taxis cluster protein CheC	Shared
AAG19986.1	transducer protein CosT; Htr5 transducer	Shared
AAG19812.1	methyl-accepting chemotaxis protein; Htr8 transducer	Shared
AAG19428.1	methyl-accepting chemotaxis protein; Htr13	Shared
AAG19381.1	Transducer protein Htr15	Shared
AAG19270.1	transducer protein Htr18	Shared
AAG19266.1	methyl-accepting chemotaxis protein; Htr4 transducer	Shared
AAG19257.1	methyl-accepting chemotaxis protein; Htr6 transducer	Shared
AAG18922.1	transducer protein MpcT; Htr14 transducer	Shared
DAC78795.1	transducer protein BasT	Shared

839 **Table 3**: Total purified RNA quality check results after TRIzol Reagent™ -based extraction. [a]See
840 Supplementary Figure 6-2 for BioAnalyzer results. Purity score below 2.0 suggest purity unsuitable
841 for RNAseq analyses.

	Liquid stationary cells			Internally inoculated halite (2 months)			Externally inoculated halite (~1 week)		
RNA quantity (µg)	1040.0	1045.2	1190.8	<20	4.4	13.9	327.6	444.0	129.6
Purity (absorbance 260/280nm)	2.10	2.09	2.08	1.95	1.54	1.61	1.99	2.03	1.98
Purity (absorbance 260/230nm)	2.44	2.38	2.47	4.67	0.96	1.44	1.89	1.78	2.05
Quality[a]	+	++	++	--	--	--	-	-	-

842

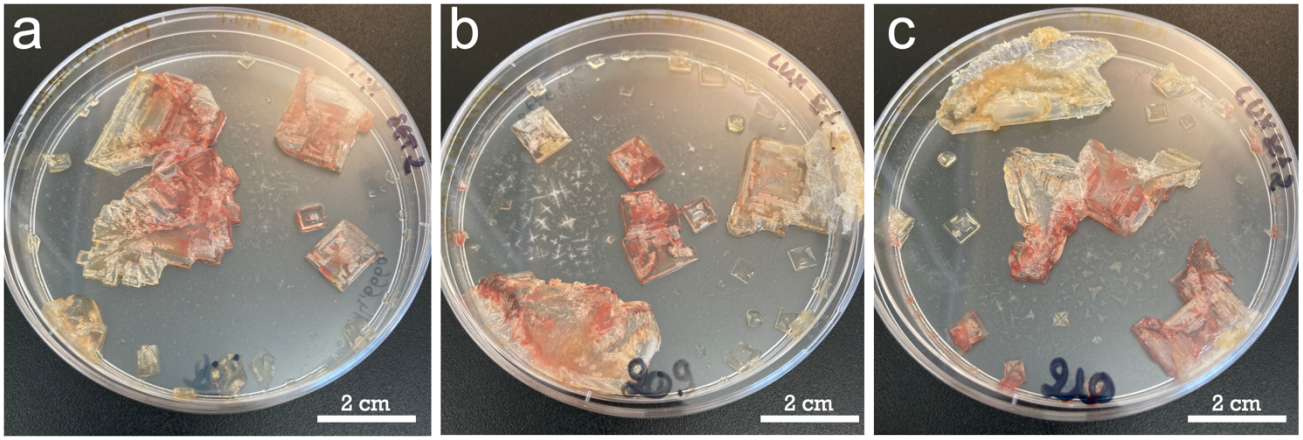

Figure 1: TNPA laboratory-grown halite crystals internally inoculated with *Halobacterium salinarum* cells observations after two months incubated at 37 °C. a) crystallization replicate 1, b) crystallization replicate 2 and c) crystallization replicate 3.

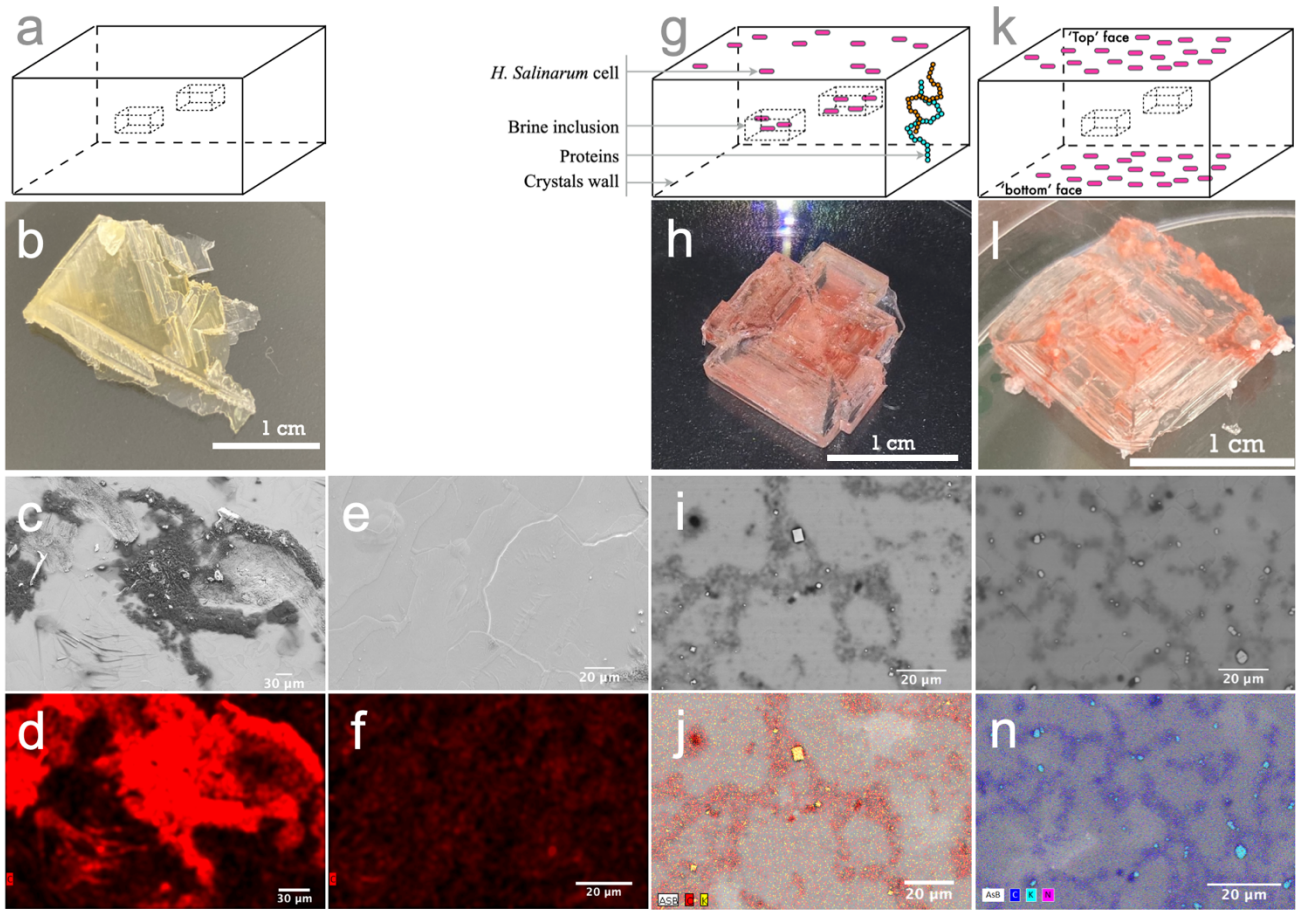

Figure 2: Laboratory-grown halite surface observation. a-f) TNPA crystals without cells. g-j) Internally inoculated TNPA crystals with *Halobacterium salinarum* cells incubated two months at 37 °C. k-n) Externally inoculated TNPA crystals with *Halobacterium salinarum* cells after approximatively one week incubated at 37 °C. a, g, k) Schematic representation of halite crystals without cells, internally inoculated and externally inoculated respectively. b-h-l) Visual observation of crystals without cells, internally inoculated and externally inoculated respectively. c, e, i, m, d, f, j, n) SEM observations and elemental composition analysis by EDX.

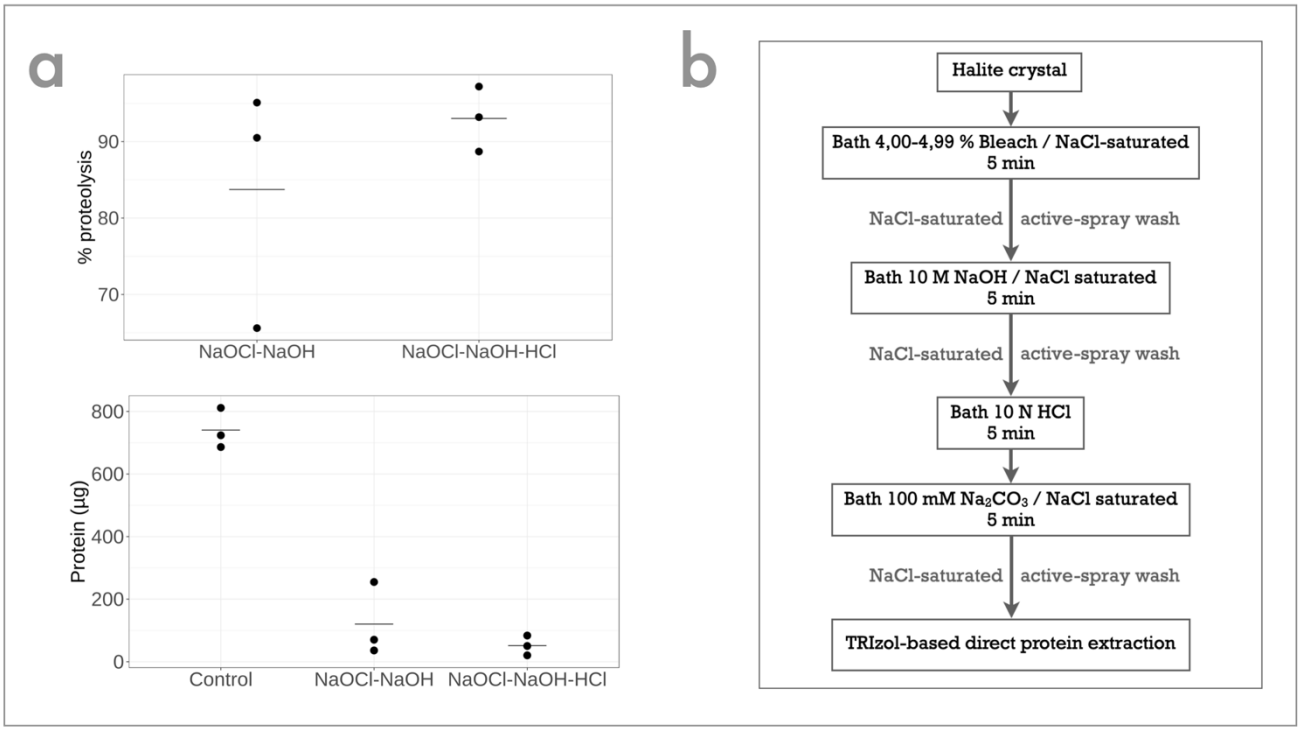

Figure 3: Surface-bounded proteins removal by chemical treatments with active-spray washes. a) Percentage of proteins lysis after NaOCl-NaOH treatment with or without additional HCl step and subsequent residual protein quantity. b) Overview of optimal NaOCl-NaOH-HCl chemical treatment with active-spray washes.

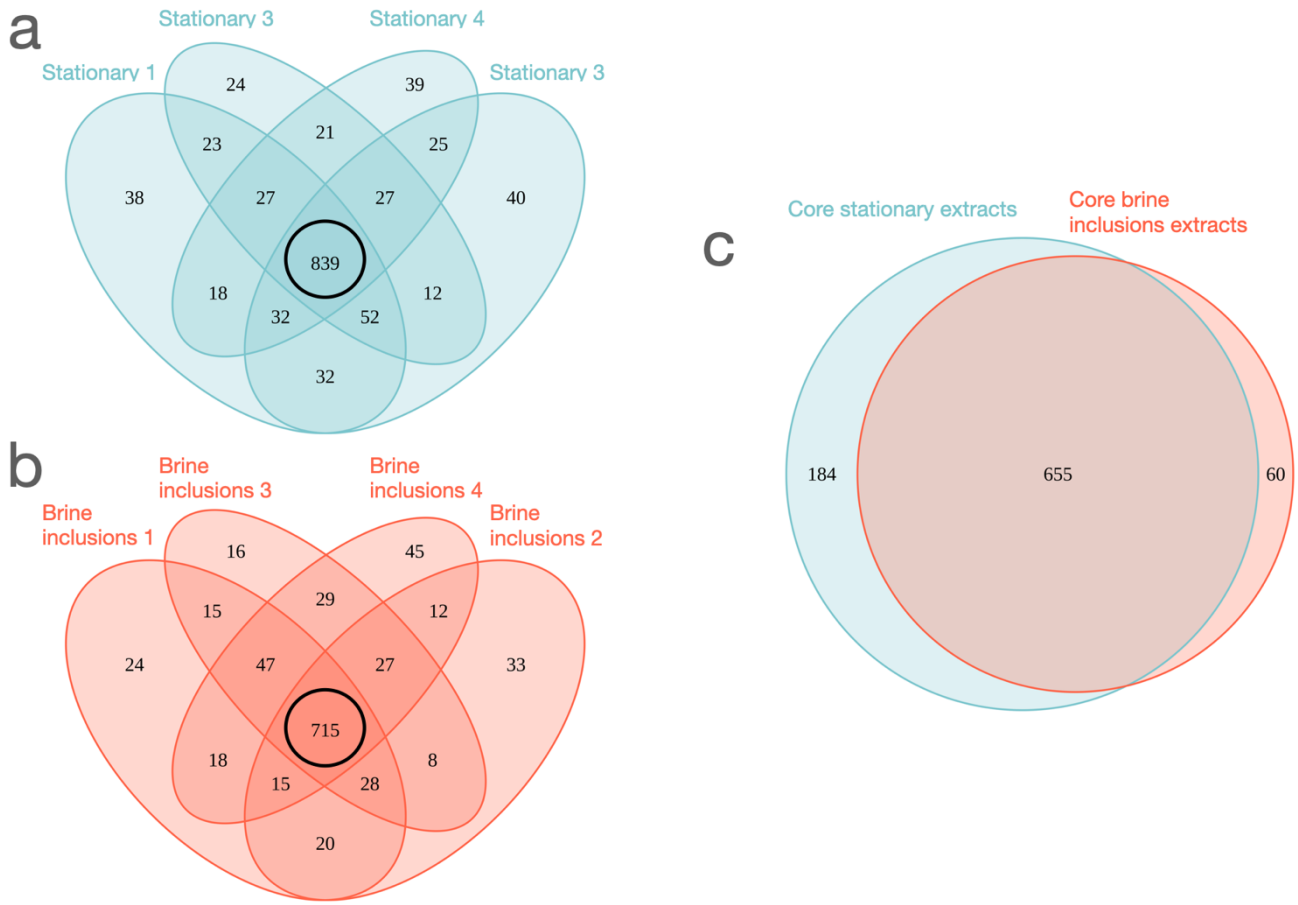

Figure 4: Venn diagrams of proteins identified by mass spectrometry for brine inclusions and liquid stationary samples. a) Comparison of biological replicates for liquid stationary extracts. b) Comparison of biological replicates for brine inclusion extracts. Black circles in a) and b) represent "core" proteins shared by the four replicates in both cases. c) Comparison of core proteins between brine inclusion extract and liquid stationary cells.

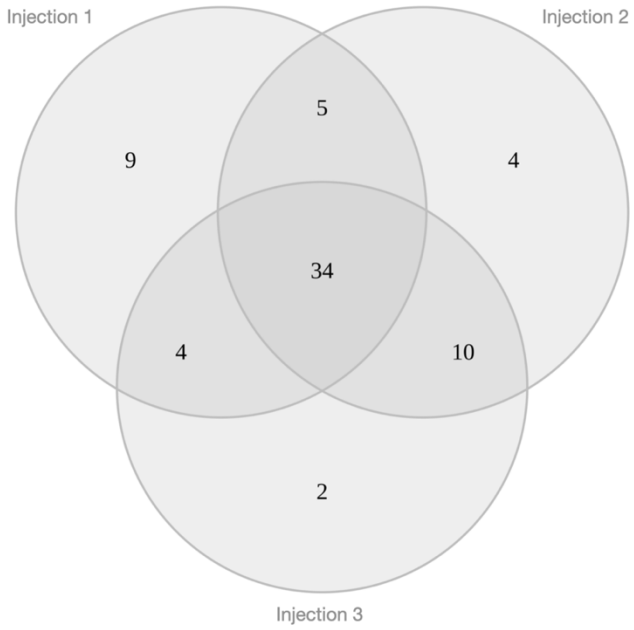

Figure 5: Venn diagram of the 68 proteins quantified by iTRAQ® with triple injection and exhibit significative differential expression in brine extracts compared to liquid stationary cultures.